Dynamic Changes in Equatorial Segment Protein 1 (SPESP1) Glycosylation During Mouse Spermiogenesis 1

Authors: Suryavathi, Viswanadhapalli, Panneerdoss, Subbarayalu, Wolkowicz, Michael J., Shetty, Jagathpala, Sherman, Nicholas E., et al.

Source: Biology of Reproduction, 92(5)

Published By: Society for the Study of Reproduction

URL: https://doi.org/10.1095/biolreprod.114.121095

BIOLOGY OF REPRODUCTION (2015) **92**(5):129, 1–16
Published online before print 11 March 2015.
DOI 10.1095/biolreprod.114.121095

Dynamic Changes in Equatorial Segment Protein 1 (SPESP1) Glycosylation During Mouse Spermiogenesis[1]

Viswanadhapalli Suryavathi,[3,4] Subbarayalu Panneerdoss,[3,4] Michael J. Wolkowicz,[4] Jagathpala Shetty,[4] Nicholas E. Sherman,[5] Charles J. Flickinger,[4] and John C. Herr[2,4]

[4]*Center for Research in Contraceptive and Reproductive Health, Department of Cell Biology, School of Medicine, University of Virginia, Charlottesville, Virginia*
[5]*Department of Microbiology, University of Virginia, Charlottesville, Virginia*

ABSTRACT

ESP1/SPESP1 **is a testis-specific, postmeiotic gene expressed in round spermatids that encodes equatorial segment protein 1, an intra-acrosomal protein found in the acrosomal matrix and on the luminal surface of the inner and outer acrosomal membranes within the equatorial segment domain of mature spermatozoa. A comparison of testicular protein extracts with caput, corpus, and caudal epididymal sperm proteins revealed striking differences in the apparent masses of SPESP1 isoforms. The predominant isoforms of SPESP1 in the testis were 77 and 67 kDa, with 47-kDa forms present to a minor degree. In contrast, SPESP1 isoforms of 47 and 43 kDa were found in caput, corpus, and caudal sperm, indicating that SPESP1 undergoes noticeable mass changes during spermiogenesis and/or subsequent transport to the epididymis. On two-dimensional (2D) SDS-PAGE, testicular SPESP1 isoforms resolved as a train of pI values from 4.9 to 5.2. Immunoprecipitated 77-kDa SPESP1 from testis reacted with the glycoprofile stain after one-dimensional and 2D gel electrophoresis, indicating that the 77-kDa testicular isoform was highly glycosylated. One charge variant of the 67-kDa isoform was also glycoprofile positive after 2D gel resolution. The 47- and 43-kDa isoforms of SPESP1 from epididymal sperm did not stain with glycoprofile, suggesting an absence of, or few, glycoprofile-sensitive glycoconjugates in epididymal SPESP1. Treatment of testicular extracts with a variety of glycosidases resulted in mass shifts in immunoreactive SPESP1, indicating that testicular SPESP1 was glycosylated and that terminal sialic acid, *N*- and *O*-glycans were present. A mixture of deglycosidase enzymes (including PNGase-F, neuraminidase, beta1–4 galactosidase, endo-alpha-*N*-acetylgalactosaminidase, and beta *N*-acetyl-glucosaminidase) completely eliminated the 77- and 67-kDa SPESP1 bands and resulted in the appearance of 75-, 60-, 55-, 50-, 47-, and 43-kDa forms, confirming that both the 77- and 67-kDa testicular forms of SPESP1 contain complex carbohydrate residues. Treatment of caudal epididymal sperm with PNGase-F enzymes showed a faint deglycosylated band at 30 kDa, but neuraminidase did not result in any molecular shift, indicating that epididymal sperm SPESP1 did not contain sialic acid/*N*-acetylglucosamine residues. These findings are consistent with the hypothesis that SPSPESP1 undergoes significant glycosylation in the testis and that the majority of these glycoconjugates are removed by the time sperm reach the caput epididymis. Studies of the fate of SPESP1 after the acrosome reaction localized SPESP1 to the equatorial segment region in both noncapacitated and capacitated, acrosome-reacted sperm. During capacitation, SPESP1 underwent proteolysis, resulting in a 27-kDa fragment. Zona-free oocytes incubated with recSPESP1 protein showed complementary binding sites on the microvillar oolemmal domain. Both recSPESP1 and anti-recSPESP1 antibody inhibited in vitro fertilization.**

acrosome, acrosome biogenesis, acrosome reaction, capacitation, deglycosylation, equatorial segment, equatorial segment protein, glycoprotein, glycosylation, oocyte, proteolysis, sperm, spermatogenesis, SPESP1, testis

INTRODUCTION

In the fertilization cascade, capacitated sperm first bind to the ovum's extracellular matrix, the zona pellucida (an event termed primary binding), and subsequently undergo the acrosome reaction, an event involving exocytosis of the anterior acrosome, leaving intact the structurally stable equatorial segment. After the acrosome reaction, sperm burrow a fertilization channel through the zona pellucida, interacting with zonal proteins in an event termed secondary binding, and enter the perivitelline space, where the sperm's equatorial segment is thought to bind with the egg plasma membrane (tertiary binding) and where the sperm and egg membranes undergo fusion, leading to sperm internalization and eventual syngamy [1]. The equatorial segment is a specialized region of the acrosome comprised of two subdomains: a region where inner and outer acrosomal membranes are closely opposed (the region of tight apposition), and a region where the inner and outer acrosomal membranes are not tightly apposed (the terminal equatorial bulb, containing acrosomal matrix). Based on electron microscopic observations of fertilization, the plasma membrane overlying the equatorial segment has been regarded as the classical site where fusion between the sperm and oolemma initiates in mammals [1–3].

Equatorial segment protein 1 (SPESP1) was first cloned and characterized in humans [4], and it has been shown to be involved in sperm-egg fusion [5]. Anti-SPESP1 antibodies inhibited sperm-egg fusion in mice [6], and sperm from mice bearing a targeted disruption of the SPESP1 gene showed a reduced ability to fuse with oocytes [7]. SPESP1 is an acrosomal matrix protein that is concentrated in the equatorial segment of mature sperm [4]. The protein is expressed selectively postmeiotically in round spermatids during acro-

[1]Supported by grant D43TW000654 from the NIH Fogarty International Center (to J.C.H.) with S.P. and V.S. holding Fogarty Postdoctoral Fellowships.
[2]Correspondence: John C. Herr, Center for Research in Contraceptive and Reproductive Health, Department of Cell Biology, School of Medicine, University of Virginia, Charlottesville, VA, 22903.
E-mail: jch7k@virginia.edu
[3]Both authors contributed equally to this manuscript.

Received: 5 May 2014.
First decision: 17 June 2014.
Accepted: 16 February 2015.

eISSN: 1529-7268 http://www.biolreprod.org
ISSN: 0006-3363

some biogenesis. A defined electron-lucent equatorial segment subdomain within the acrosomal matrix of human sperm may be identified as early as the acrosomal vesicle stage (Golgi phase) of acrosome biogenesis using SPESP1 as a biomarker [4], allowing the equatorial segment subdomain to be traced through various phases of acrosome formation, including Golgi, cap, acrosome elongation, and acrosomal matrix condensation, during the steps of spermiogenesis [4].

The plasma membrane overlying the equatorial segment has been studied in mice, rats, and humans using freeze-fracture [8–10], surface replica [11], and atomic force microscopy techniques [12], revealing structural features that distinguish it from the plasma membrane overlying the anterior acrosomal and postacrosomal domains. The remarkable molecular architecture of the region of tight apposition within the equatorial segment is characterized by a heterogeneous population of both small and large intramembranous particles [8].

Several molecules have been localized to the equatorial segment [13] domain (lying within the acrosomal matrix, inner and outer acrosomal membranes, adjacent cytoplasm, and/or overlying plasmalemma), including CALM1 [14], actin [15, 16], annexins ANXA1 and ANXA2 [17], and heat shock proteins HSPA1A (Hsp70) and HSP90AA1 (Hsp90) [18, 19]. Molecules that mediate fusion have generally been considered to be localized in the plasma membrane overlying the equatorial segment or possibly within the exposed acrosomal matrix that occupies the cleft in acrosome-reacted sperm between the inner and outer acrosomal membranes of the equatorial segment. Because sperm are not able to fuse with the egg before the acrosome reaction, the molecules responsible for fusion likely are not available in a fusigenic state on the membrane overlying the equatorial segment of noncapacitated, nonacrosome-reacted sperm.

One protein has been identified as being restricted to the sperm and unique to the equatorial segment. The equatorin protein (MN9 antigen) was identified in mice and found to be conserved in mammals, including humans, and selectively localized to the equatorial segment region of mature sperm [20]. Gametes incubated with anti-equatorin (MN9 antibody) showed defective fertilization. In particular, sperm-egg fusion and release of cortical granules and early egg activation were especially affected; however, no effects were seen on zona pellucida binding or zona penetration [21] either in vivo or in vitro [22]. Electron microscopic studies led to the conclusion that during the acrosome reaction, equatorin translocates to the plasma membrane overlying the equatorial segment [23].

To date, investigations of SPESP1 have focused on the molecule's temporal appearance during spermiogenesis and the role of SPESP1 in sperm-egg interaction and fertilization, but to our knowledge, detailed biochemical characterization of SPESP1 protein isoforms has not been reported. In contrast to previous studies [7] that concluded SPESP1 is no longer detected in the equatorial segments of acrosome-reacted sperm, the present study provides evidence that SPESP1 is localized in the equatorial region of mouse spermatozoa and is retained in this domain during capacitation and following exocytosis of the anterior acrosome. Importantly, mouse SPESP1 is shown to be polymorphic and highly glycosylated and to undergo deglycosylation before sperm reach the epididymis, leading to a new hypothesis that acrosome biogenesis is accompanied by deglycosylation. This hypothesis may have broad significance for understanding the basic cell biology of luminal condensation of some types of secretory vesicle proteins.

MATERIALS AND METHODS

Cloning and Expression of Murine SPESP1 from Mouse Testicular cDNA

Utilizing the human SPESP1 (hSPESP1) gene, the National Center for Biotechnology Information Basic Local Alignment Search Tool (BLAST) database was queried, and a murine transcript (accession no. AK015620) demonstrating 81% homology to the hSPESP1 gene was found. Two gene-specific primers designed from the nucleotide sequence were used to amplify by PCR the full-length murine SPESP1 (mSPESP1) from a mouse testis cDNA library (BD Biosciences Clontech). PCR products were separated on agarose gels, and bands of expected molecular sizes were gel eluted and subcloned in pCR2.1 TOPO vector (Invitrogen). Multiple cDNA clones were sequenced in both directions using vector-derived primers on a PerkinElmer Applied Biosystems DNA sequencer (Biomolecular Research Facility, University of Virginia). Expression of a recombinant SPESP1 (recSPESP1) protein with a C-terminus His tag was achieved by designing both forward and reverse gene-specific primers containing *Pci*I and *Xho*I restriction sites, respectively, and amplifying the mature form of mSPESP1 lacking the signal peptide from the previously isolated mouse testis cDNA library transcript. The *Pci*I site simultaneously contains an ATG start codon and a ''sticky-ended,'' ligation-compatible *Nco*I site. It should be noted that both half-sites are lost upon successful ligation. PCR products were separated on agarose gels, and a band of approximately 800 bp was isolated and subcloned in pCR2.1 TOPO vector. After confirming the sequence, the insert was restriction digested, gel purified, directionally ligated into predigested (*Nco*I and *Xho*I) pET28b(+) vector, and used to transform competent NovaBlue (DE3) cells (Invitrogen). The bacterial cultures from single colonies were grown to an optical density of 0.8 at 600 nm at 37°C in Luria broth in the presence of 50 μg/ml of ampicillin. Isopropyl-β-D-thiogalactopyranoside (IPTG; Sigma) was then added to a final concentration of 1 mM to induce expression. After 3 h of induction, the bacteria were collected by centrifugation. The bacterial pellet was extracted in Bugbuster Protein Extraction Reagent (Novagen) containing benzonase nuclease (Novagen), chicken lysozyme (Sigma), and a protease inhibitor cocktail (Roche). The cell extract was centrifuged at 15 000 × *g*, and recombinant protein was purified from the supernatant on a His-binding., Ni^{2+} chelation-affinity resin column following the instructions from the manufacturer (Novagen). This was followed by Prep Cell (Bio-Rad) isolation to homogeneity, and subsequently, the eluates were dialyzed overnight against three changes of PBS. The dialyzed protein was stored at −80°C until use.

Generation of SPESP1 Polyclonal Antibody

Polyclonal antibody to mSPESP1 was raised in guinea pigs against the purified recSPESP1 polypeptide. The purified mSPESP1 recombinant protein was homogenized in PBS and emulsified with an equal volume of complete Freund adjuvant. Approximately 30 μg of the affinity- and Prep Cell-purified recombinant protein were injected subcutaneously into each guinea pig. Control animals were injected with Freund's adjuvant alone. Animals were boosted three times at intervals of 14 days with 30 μg of the recombinant protein in incomplete Freund adjuvant, and serum was collected 7 days after each boost. The guinea pigs were euthanized according to the Institutional Animal Care and Use Committee Guidelines of the University of Virginia for collection of the antiserum.

Preparation of Mouse Sperm and In Vitro Capacitation

Mice were handled and euthanized according to the guidelines of the Institutional Animal Care and Use Committee of the University of Virginia. Caput, corpus, and cauda epididymis from ICR mice were separated, and spermatozoa were collected by teasing the tissues into Whitten HEPES-buffered medium (WH). Fewer sperm were routinely released from the caput and corpus compared to the cauda epididymis; thus, after sperm washing, equal amounts of epididymal sperm extracts were loaded into each well. In vitro capacitation was carried out as described previously [24, 25]. Briefly, sperm were collected and washed in WH medium [24, 26, 27] containing 100 mM NaCl, 4.7 mM KCl, 1.2 mM KH_2PO4, 1.2 mM $MgSO_4$, 5.5 mM glucose, 1 mM pyruvic acid, and 4.8 mM L(+)-lactic acid hemicalcium salt in 20 mM HEPES (pH 7.3). Sperm pellets were resuspended in WH medium at 2×10^6 sperm/ml and incubated at 37°C and 5% CO_2 in air. Capacitating medium consisted of 5 mg/ml of bovine serum albumin (BSA) and 10 mM $NaHCO_3$ in WH medium. In all cases, pH was maintained at 7.3. Spermatozoa were capacitated for 90 min. After capacitation, the acrosome reaction was induced by supplementing the medium with calcium ionophore A23187 (Sigma) to a final concentration of 5 μg/ml (from 5 mg/ml stock solution in dimethyl

sulfoxide) and incubating sperm for 30 min at 37°C under 5% CO_2 [24, 26, 28]. For noncapacitation controls, spermatozoa were collected at time zero.

recSPESP1-Binding Domain in Metaphase II-Arrested Oocytes

Metaphase II eggs were obtained from ICR female mice (age, 8–10 wks) that were superovulated by injection of 5 IU of equine chorionic gonadotropin (Sigma) followed 48 h later by 5 IU of human chorionic gonadotropin (hCG; Sigma). Eggs were collected from the oviducts 16 h post-hCG and were washed with TYH medium [28]. Cumulus cells were removed with 0.1% bovine testis hyaluronidase (Sigma). In experiments requiring eggs without zona pellucida, the eggs were treated with Tyrode acidic solution (Sigma), and zona-free eggs were then washed in Tyrode-lactate solution (Sigma) and left to recover in fertilization medium (TYH medium) for at least 1 h at 37°C in a 5% CO_2 incubator. Zona-free oocytes were incubated with 5% normal goat serum (NGS)/medium for 30 min. Oocytes were washed five times in TYH medium and incubated with 100 μg/ml of recSPESP1 for 60 min at 37°C and 5% CO_2. They were then washed five times and incubated with guinea pig anti-recSPESP1 polyclonal antibody (1:100) in 5% NGS/medium for 1 h at 37°C and 5% CO_2. Oocytes were washed five times and incubated with fluorescent-conjugated goat anti-guinea pig antibody (1:200; Jackson ImmunoResearch) in 5% NGS/medium for 1 h at 37°C and 5% CO_2. The specimens were washed and incubated with Hoechst nuclear stain and visualized under a Zeiss standard fluorescence microscope.

In Vitro Fertilization

In vitro fertilization (IVF) was performed as previously described [28]. To study the effect of anti-recSPESP1 serum, sperm were incubated with decomplemented (56°C, 30 min) immune or nonimmune serum. Zona-intact oocytes were incubated in fertilization medium with immune/nonimmune serum and with or without recSPESP1 protein for 60 min before coincubation. Capacitated sperm (10^5/ml) were then added into each oocyte-containing drop. After 6 h of coincubation, oocytes were washed in fertilization medium to remove loosely bound sperm and incubated in embryo culture medium for 24 h, and 2-cell embryos were scored for determination of fertilization. In addition, Hoechst nuclear stain was used to distinguish 1-cell embryos containing both male and female pronuclei from unfertilized oocytes (with metaphase II-arrested nuclei).

Indirect Immunofluorescence of Sperm

Mouse sperm (both capacitated and noncapacitated) were air-dried on slides, fixed with 4% paraformaldehyde in PBS for 20 min at room temperature, and washed with PBS (four washes for 5 min each). After fixation, the sperm were permeabilized with ice-cold methanol for 7 min, washed with PBS (four washes for 5 min each), and blocked with 10% NGS in PBS for 60 min at room temperature. Sperm cells were then incubated with guinea pig antiserum against mSPESP1 diluted (1:200) in PBS containing 1% NGS for 1 h at room temperature. After the primary antibody incubation, the sperm cells were washed with PBS (four washes) and incubated with fluorescein isothiocyanate-conjugated anti-guinea pig secondary antibody diluted (1:200) in 1% NGS in PBS for 1 h at room temperature. The secondary antibody treatment was followed by four washes in PBS, treatment with DAPI-SlowFade Light (Molecular Probes), and observation by phase-contrast and epifluorescence microscopy using an Axiophot microscope (Carl Zeiss, Inc.). Peanut agglutinin (PNA) lectin (1:100) was used to analyze the status of the acrosome. Controls included nonimmune serum and secondary antibody alone.

For live staining, after 60 min of capacitation, caudal epididymal sperm were probed with immune or nonimmune serum for 1 h, washed three times, and incubated with secondary antibody as described above. Sperm were then stained with PNA lectin as described above and scored for PNA staining. PNA-positive anterior acrosomes were scored as acrosome intact, whereas PNA-negative sperm were scored as acrosome reacted. The colocalization of SPESP1 was determined in PNA-positive and PNA-negative populations. One-hundred sperm were scored for PNA and SPESP1 staining. Sperm nuclei were stained with Hoechst 33342 (Molecular Probes), and cells were observed under a Nikon Eclipse 80i microscope.

Western Blot Analysis

Proteins from testis and spermatozoa were extracted in RIPA buffer (Thermo Scientific) for immunoprecipitation in NP-40 (20 mM Tris-HCl [pH 8], 137 mM NaCl, 10% glycerol, 1% Nonidet P-40, and 2 mM ethylenediaminetetra-acetic acid) for deglycosylation experiments and in Celis buffer (9.8 M urea, 2% Nonidet P-40, and 100 mM dithiothreitol) for two-dimensional (2D) analysis. All extraction buffers were supplemented with protease inhibitor cocktail (Roche), and total protein was quantified using the Bradford assay (Thermo Scientific). Samples were loaded onto precast 10.5%–14% Criterion SDS-PAGE gels (Bio-Rad) and electrotransferred onto nitrocellulose membranes (pore size, 0.2 μm; Bio-Rad), and membranes were stained with Ponceau-S to confirm the protein transfer. The membranes were blocked with 5% nonfat dry milk in 0.05% Tween 20 and PBS for 1 h at room temperature and probed with guinea pig anti-mouse SPESP1 antibody at 1:3000 dilution in 5% blocking reagent for 1 h. The blots were incubated with a horseradish peroxidase-conjugated goat anti-guinea pig immunoglobulin (Ig) G antibody (The Jackson Laboratory) at a dilution of 1:5000 to 1:7500 in PBS containing 0.01% Tween 20 for 1 h. The membranes were developed using TMB substrate (KPL). The histidine-tagged recSPESP1 was detected using anti-His tag monoclonal antibody.

Immunoprecipitation of SPESP1 in Testis and Sperm

Immunoprecipitation was carried out using the Immunoprecipitation Kit (Roche Applied Science). RIPA protein extracts of mouse testis (3 mg in 1 ml) or sperm (700 μg in 1 ml) were incubated with a 1:100 dilution of guinea pig anti-mouse SPESP1 antibody and gently rocked for 4 h at 4°C. A homogeneous protein-A agarose suspension (70 μl) was added to the mixture and incubated overnight at 4°C on a rocking platform. Immune complexes were collected by centrifugation at 12 000 × *g* for 30 sec in a microcentrifuge. After careful removal of supernatants, 1 ml of wash buffer 1 (50 mM Tris-HCl, 150 mM NaCl, 1% NP-40, and 0.05% sodium deoxycholate) was added, and the beads were resuspended and incubated for 20 min at 4°C on a rocking platform. This washing process was repeated with wash buffer 2 (50 mM Tris-HCl, 500 mM NaCl, 0.1% NP-40, and 0.05% sodium deoxycholate) and wash buffer 3 (10 mM Tris-HCl, 0.1% NP-40, and 0.05% sodium deoxycholate), and complexes were collected and solubilized with 75 μl of 2× Laemmli sample buffer. Proteins were denatured by heating to 100°C for 10 min. Protein-A agarose was removed by centrifugation at 12 000 × *g* for 60 sec at room temperature in a microcentrifuge, and aliquots were analyzed by SDS-PAGE and Western blotting.

2D Gel Electrophoresis

Mouse testicular immunoprecipitates (both immune and nonimmune) were eluted from protein-A agarose beads with Celis extraction buffer containing protease inhibitors (Roche) and resolved by 2D gel electrophoresis [25, 29, 30]. SPESP1 eluates were loaded onto IPG strips (pI 3–10 nonlinear immobilized pH gradient; Bio-Rad) and were subjected to passive rehydration for 3 h at room temperature and active rehydration overnight at 50 V followed by isoelectric focusing at 25 000 Vh. The IPG strips were then loaded on the second dimension 10%–14% gradient SDS-PAGE gels (Bio-Rad). Proteins were transferred onto nitrocellulose membranes for immunoblotting.

Glycosylation Site Analyses by Mass Spectrometry

Immunoprecipitated mouse testicular and sperm SPESP1 isoforms were analyzed by one-dimensional (1D) and 2D SDS-PAGE. Gels were fixed, stained with glycoprofile fluorescent stain (Sigma) according to manufacturer's instructions, and observed under ultraviolet transillumination. The glycosylation positive bands (1D gels) or spots (2D gels) were cored and subjected to mass spectrometry to authenticate SPESP1 amino acid sequences. In addition, protein sequences were analyzed by mass spectrometry for signs of in vivo deglycosylation (Asparagine-X-Ser/Thr to Aspartic acid-X-Ser/Thr). This is a consensus sequence for *N*-linked protein glycosylation [31]. Positive controls consisted of the glycosylated proteins ovalbumin (45 kDa) and RNase (17 kDa) (PTM Marker; Sigma), which were used as standards.

Enzymatic Deglycosylation of Proteins

Glycosidase treatments of testicular and sperm protein extracts were performed with peptide *N*-glycanase-F (PNGase-F), neuraminidase, endo-α-*N*-acetylgalactosaminidase, β1–4 galactosidase, β-*N*-acetylglucosaminidase, and a combination of these enzymes (Glycomix) as well as a combination of neuraminidase and PNGase-F. Protocols and buffers supplied by the manufacturer (New England BioLabs) were used. In the basic form of the experiment, testicular and caudal epididymal sperm proteins were extracted with NP-40 lysis buffer and incubated overnight with each enzyme at 37°C. Control samples were incubated in reaction buffers without glycosidases.

For PNGase-F, deglycosylation proteins were extracted from testis and sperm using NP-40 lysis buffer supplemented with complete protease inhibitor

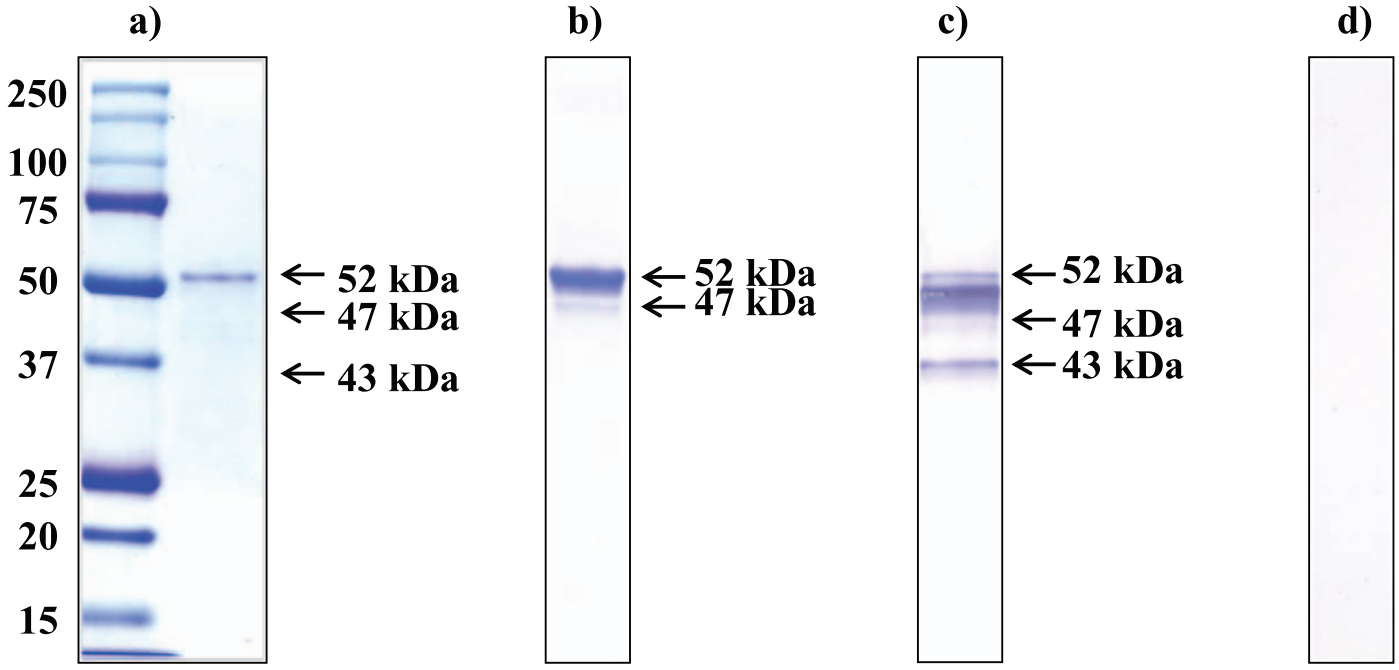

FIG. 1. Purified recSPESP1 and antiserum specificity. **a**) Coomassie blue-stained SDS-PAGE gel of 100 ng of Ni-affinity-purified, His-tagged mouse SPESP1 (expressed in BL21-DE3 cells) showing the major 52-kDa recombinant protein. **b**) Purified SPESP1 transferred to nitrocellulose membrane and probed with anti-His tag antibody immunoreacted with the 52-kDa band and a fainter 47-kDa band. **c**) RecSPESP1 probed with anti-recSPESP1 immune serum recognized a 52-kDa band as well as 47- and 43-KDa bands. **d**) Nonimmune serum-probed membrane containing recSPESP1 showed no immunoreactivity.

(Sigma). Testis (20 μg) or sperm (10 μg) extracts were combined with 1 μl of 10× glycoprotein denaturing buffer and H_2O to make a total reaction volume of 10 μl. Glycoproteins were denatured by heating the samples at 95°C for 5 min, followed immediately by placing samples on ice and then a brief centrifugation at 16 000 × g for 10 sec. Next, 2 μl of 10× G7 Reaction Buffer, 2 μl of 10% NP-40, and 6 μl of H_2O were added to the sample to reach a total reaction volume of 20 μl, to which 1 μl of PNGase-F (catalog no. P0704S; New England BioLabs) was added. Samples were mixed gently and incubated at 37°C overnight.

For deglycosylation mix (catalog no. P6039; New England BioLabs, Inc.), testis and sperm lysates were incubated with 2 μl of 10× glycoprotein denaturing buffer, heated at 100°C for 10 min, placed on ice, and centrifuged as described above for 10 sec. To the denatured glycoprotein reaction were added 5 μl of 10× G7 Reaction Buffer, 5 μl of 10% NP-40, 15 μl of H_2O, and 5 μl of deglycosylation enzyme cocktail. The sample was gently mixed and incubated at 37°C overnight.

In the case of endo-α-*N*-acetylgalactosaminidase (catalog no. P0733S; New England BioLabs, Inc.), testis and sperm lysates were denatured with 1 μl of 10× glycoprotein denaturing buffer, heated for 5 min at 95°C, chilled on ice, centrifuged as described above, and then combined with 10× G7 Reaction Buffer (4 μl), NP-40 (4 μl), and 2 μl of endo-α-*N*-acetylgalactosaminidase.

For the other glycosidases, testis or sperm lysates were incubated with 1 μl of 10× G1 Reaction Buffer and neuraminidase (catalog no. P0720S; New England BioLabs, Inc.), β1–4 galactosidase (catalog no. P0730S; New England BioLabs, Inc), β-*N*-acetylglucosaminidase (catalog no. P0732S; New England BioLabs, Inc.), and glycol at 37°C overnight. The control samples were incubated without these glycosidases. Following these enzymatic treatments, experimental samples were analyzed for changes in SPESP1 mass by SDS-PAGE-Western blot analysis with mouse anti-SPESP1 antibody.

RESULTS

Expression of recSPESP1 Protein and Generation of Polyclonal Anti-SPESP1 Antibody

SPESP1 cDNA was amplified from an adaptor ligated murine testicular cDNA library. The SPESP1 open reading frame encoded a 399-amino-acid protein, and the full-length recSPESP1, including amino acids 1–399 and a C-terminal His_6-tag, was expressed in *Escherichia coli*. Upon induction with IPTG for 3 h, the bacterial cells were analyzed by SDS-PAGE with an anti-His tag antibody, and a major recSPESP1 protein migrating at 52 kDa was observed on Coomassie gels (data not shown). The recSPESP1 protein was then purified to homogeneity by Ni-affinity chromatography followed by Prep Cell isolation and was subsequently used to immunize guinea pigs. Purity of the recSPESP1 preparation was analyzed by 1D electrophoresis, and the gel was stained with Coomassie blue (Fig. 1a), revealing a prominent 52-kDa band as well as very faint minor bands. Probing with anti-His antibody, both the prominent 52-kDa band (Fig. 1b) as well as the less abundant 47-kDa band immunoreacted, demonstrating the presence of the C-terminal His-tag. This indicated that the recSPESP1 preparation used in the present study was highly purified. Blots containing the purified mouse SPESP1 recombinant protein were probed with the guinea pig anti-mouse SPESP1 polyclonal serum raised to this preparation, revealing immunoreactivity with the major 52-kDa SPESP1 band (Fig. 1c) as well as the minor 47- and 43-kDa SPESP1 bands. Although the expected molecular weight of SPESP1 deduced from primary sequence is 44.7 kDa, recombinant bacterial SPESP1 ran at the higher (52 and 47 kDa) apparent masses, whereas nonimmune control blots showed no signal (Fig. 1d). Due to absence of anti-His immunoreactivity with the 43-kDa band but staining with the anti-SPESP1 antisera, the 43-kDa form likely lacks a C-terminus.

SPESP1 Protein Isoforms in Testis and Epididymal Sperm

SPESP1 protein masses were studied in protein extracts of the testis and in sperm collected from the caput, corpus, and cauda epididymis. Testicular SPESP1 showed predominantly 77- and 67-kDa masses, whereas epididymal sperm extracts from caput, corpus, and cauda all showed similar 47- and 43-kDa SPESP1-immunoreactive bands (Fig. 2). Identical membranes probed with nonimmune sera showed no immunoreac-

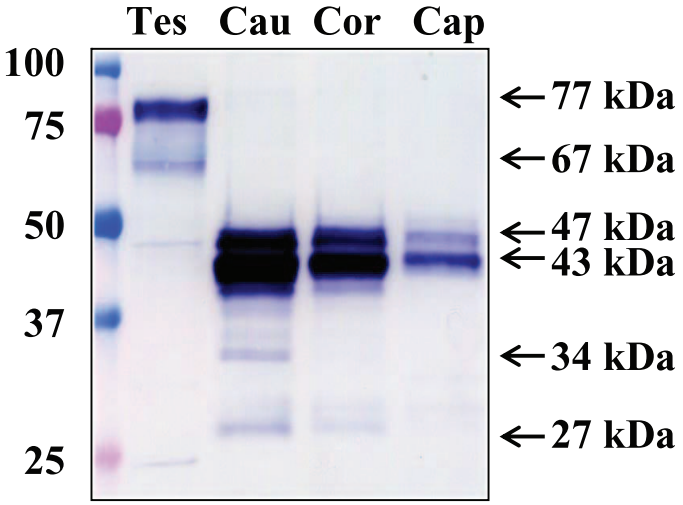

FIG. 2. Western blot analysis of SPESP1 in testis and epididymis. Caput (lane cap), corpus (lane cor), and caudal (lane cau) epididymal sperm all showed immunoreactive SPESP1 bands of 47 and 43 kDa, whereas testicular protein extracts (lane Tes) revealed major 77- and 67-kDa immunoreactive SPESP1 bands, which were absent in epididymal sperm, as well as a minor 47-kDa SPESP1 band.

tivity (Supplemental Fig. S1; all Supplemental Data are available online at www.biolreprod.org). The sperm samples from each epididymal region notably lacked the high-molecular-weight, 77- and 67-kDa immunoreactive bands observed in the samples from testis. From these observations, it may be concluded that the processes by which the high-molecular-weight, 77- and 67-kDa SPESP1 isoforms transform to lower mass proteins occurs principally within the testis before sperm reach the epididymis.

Careful analysis of the testicular protein extracts revealed that although the predominant protein isoforms of SPESP1 in the testis were 77 and 67 kDa, testicular extracts contained a fainter 47-kDa band that comigrated with the 47-kDa SPESP1 band from the epididymal samples (Fig. 2). These observations suggested that SPESP1 proteins from the testis consisted predominantly of high-molecular-weight isoforms, but testis samples also contained a subpopulation of SPESP1 that had changed from the higher-molecular-weight, 77- and 67-kDa forms to the 47-kDa form before reaching the caput epididymis.

Interestingly, corpus and cauda sperm extracts showed additional minor immunoreactive SPESP1 bands between 40 and 27 kDa. These could be proteolyzed products of SPESP1 (Fig. 2). Immunoprecipitation of sperm SPESP1, precise excision, and mass spectrometry microsequencing of the 37- and 34-kDa bands yielded six and four SPESP1 peptides, respectively, confirming these as authentic SPESP1 proteins and supporting their possible derivation by proteolysis (Supplemental Fig. S2, c–f). Blots probed with nonimmune serum did not show any immunoreactivity (Supplemental Fig. S1). It was noted that the intensity of the 47-, 43-, and 27-kDa sperm bands (Fig. 2) was greater in samples from cauda than caput.

Immunoprecipitation of Testicular and Sperm SPESP1 and Authentication by Mass Spectrometry Microsequencing

SPESP1 was immunoprecipitated from mouse testis and sperm and analyzed by SDS-PAGE-Western blotting, and a portion of each gel was silver stained. Based on immunoreactive bands on the Western blot, corresponding silver-stained bands of 77 kDa from testis and 47, 43, 37, and 34 kDa from sperm were cored from the gel, digested with trypsin, and analyzed by mass spectrometry, yielding a range of SPESP1 peptides (Supplemental Fig. S2, a–f). This recovery of SPESP1 peptides (highlighted in yellow) confirmed that both the high- and low-molecular-weight immunoreactive bands identified in testis and sperm were authentic SPESP1 proteins.

Analysis of the amino acid residues at each end of the peptides recovered from both testicular and sperm SPESP1 (Supplemental Fig. S2) revealed that all peptides were bounded by arginine or lysine residues, confirming their tryptic origins. Tryptic peptides derived from the N-terminal 134 amino acids of SPESP1 were notably absent from the analysis of both testicular and sperm protein digests, although lysines 2, 49, 55, 56, and 74 and arginines 61, 69, 96, 105, 107, 112, 113, 114, 115, and 125 are present in this N-terminal domain and are predicted to be potential cleavage sites. A peptide that began after lysine 142 was the most N-terminal sequence to be recovered from the digest of the 77-kDa testicular SPESP1, whereas other peptides recovered from testicular SPESP1 spanned sequences extending to the very C-terminal proline 399. Tryptic peptides beginning after arginine 134 were recovered from both the 47- and 43-kDa immunoprecipitated sperm SPESP1 bands. However, peptides spanning amino acids 370–399 at the C-terminus were not detected in the sperm preparations, although they were present in the 77 testicular SPESP1, suggesting that a C-terminal proteolysis event might occur.

Evidence for SPESP1 Glycosylation

One explanation for the higher-molecular-weight forms of SPESP1 in the testis might be glycosylation. Bioinformatic analysis using NetOGlyc 3.1 showed two potential *N*-linked (Supplemental Fig. S3) and 18 potential *O*-linked glycosylation sites in SPESP1. To test if SPESP1 is a glycoprotein, both testicular and sperm SPESP1 were immunoprecipitated and confirmed by Western blot analysis (Fig. 3, a and b), and the glycoprofile stain was employed to identify glycoproteins on a 1D gel loaded with SPESP1 immunoprecipitates (Fig. 3, c and d). Western blot analysis confirmed that prominent SPESP1 bands were immunoprecipitated from both testis (77 and 67 kDa) (Fig. 3a) and sperm (47 and 43 kDa) (Fig. 3b). Glycoprofile staining showed that the 77-kDa SPESP1 band from testis was glycopositive (Fig. 3c, white asterisk). Interestingly, although they were very abundant in immunoprecipitates when stained with anti-SPESP1 antibody (Fig. 3b), neither the 47- nor the 43-kDa SPESP1 bands from the sperm were positive with the glycoprofile stain in the 1D SDS-PAGE (Fig. 3d), suggesting that these epididymal sperm SPESP1 isoforms contain few oligosaccharides. Known to be glycosylated in the CH2 domain on the Fc fragment [32], heavy chains from IgG in the immunoprecipitates were strongly glycopositive and served as an endogenous positive-control glycoprotein.

Testicular SPESP1 was immunoprecipitated, and immune complexes were eluted with Celis buffer and analyzed using 2D SDS-PAGE to resolve glycosylated isoforms for spot coring and mass spectrometry. Western blot analysis with anti-SPESP1 antibody revealed a series of SPESP1 charge variants at 77 and 67 kDa (Fig. 3e, red circle) and a few spots at 47 and 43 kDa (Fig. 3e, black circle). Nonimmune immunoprecipitates did not show any immunoreactivity (Supplemental Fig. S4). Having confirmed by Western blot analysis that SPESP1 had been immunoprecipitated (Fig. 3e), a parallel gel was stained with glycoprofile and showed four positive glycoprotein spots (two major and two minor) at 77 kDa, ranging from pI 4.9 to pI 5.2, and one minor positive spot at 67 kDa, in the range of pI

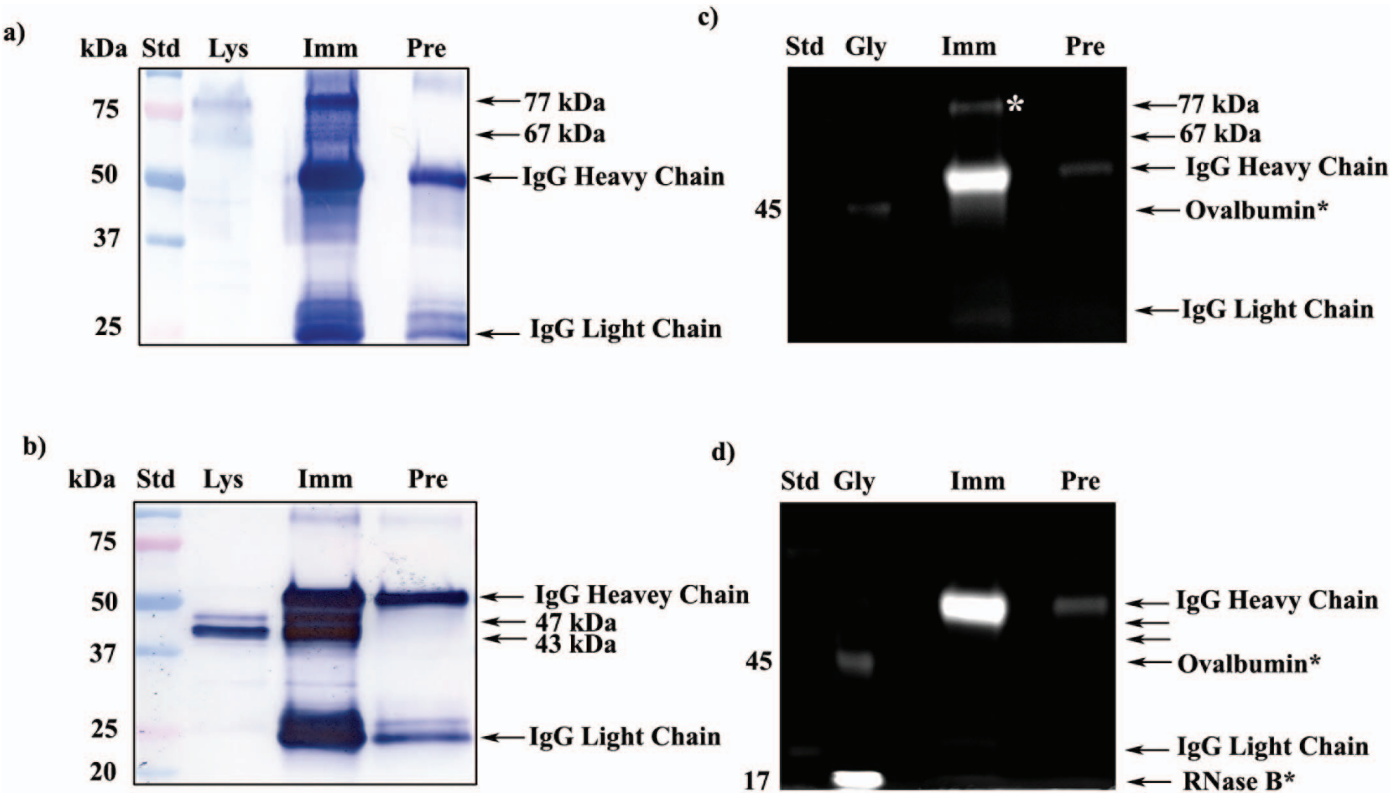

FIG. 3. Glycoprofile staining of immunoprecipitated mouse testicular and sperm SPESP1. **a**) 1D Western blot probed with anti-SPESP1 serum shows 77- and 67-kDa SPESP1 isoforms in the starting testicular lysate (Lys). These isoforms were enriched in testicular immune complexes precipitated with immune (Imm) but not with nonimmune (Pre) sera. **b**) 1D Western blot of sperm lysate (Lys) revealed SPESP1 proteins at 47- and 43-kDa, which were enriched only in the immune, not in the nonimmune, immunoprecipitates. **c**) The 77-kDa testicular SPESP1 band (white asterisk) reacted with the glycoprofile stain only in the lane with immune serum precipitate. **d**) Neither the 47- nor the 43-kDa sperm band reacted positively with glycoprofile stain. **c** and **d**) In glycoprofile-stained gels, 56-kDa IgG heavy chains were stained in both immune and nonimmune lanes in accord with the known heavy-chain glycosylation at Asn297 [37]. Glycoprotein standards (Gly) ovalbumin at 45 kDa (**c** and **d**) and RNase at 17 kDa (**d**) were glycostain positive. **e**) SPESP1 isoforms immunoprecipitated from mouse testis were analyzed by 2D SDS-PAGE Western blot using SPESP1 antibody, revealing trains of SPESP1 charge variants at 77 and 67 kDa (red circle); 47 and 43 kDa (black circle). **f**) Several 77-kDa SPESP1 charge variants and one 67-kDa variant stained with glycoprofile. Nonimmune immunoprecipitates probed with SPESP1 immune serum showed only heavy and light chains (Supplemental Fig. S4). Std, Standard.

4.9. One of the 77-kDa glycopositive spots (Fig. 3f) was cored under the ultraviolet transilluminator and sent for mass spectrometry microsequencing, resulting in the recovery of 14 peptides (Supplemental Fig. S2b) unique to SPESP1 and providing additional confirmation that testicular SPESP1 was glycosylated.

Deglycosylation and Mobility Shifts in Mouse Testicular SPESP1

Because SPESP1 was predicted to possess two well-conserved *N*-glycosylation (N128 and N278) sites (Supplemental Fig. S3) as well as *O*-glycosylation sites, testicular and sperm extracts containing SPESP1 were treated with glycosidases and examined for changes in apparent molecular weights using Western blot analysis with SPESP1-specific polyclonal antibodies.

An amidase, PNGase-F cleaves between the innermost GlcNAc and asparagine residues of high-mannose, hybrid, and complex oligosaccharides from *N*-linked glycoproteins [33], whereas neuraminidase removes sialic acids from *O*-linked sugars [34]. In Western blots of PNGase-F-treated testis samples, the upper 77-kDa SPESP1 band became less prominent, and a 60-kDa band appeared, an apparent molecular weight shift of approximately 17 kDa (Fig. 4a). Neuraminidase-treated testis samples showed a shift of approximately 7 kDa, with the upper 77-kDa SPESP1 band being reduced to 70 kDa and the lower 67-kDa band not showing any change in apparent molecular weight (Fig. 4b). Interestingly, neither of these enzymes deglycosylated all of the 77-kDa band, suggesting that SPESP1 could be a polyglycoprotein with both *N*- and *O*-linked residues. Next, treatment with endo-α-*N*-acetylgalactosaminidase resulted in the appearance of 50-, 47-, and 43-kDa bands (Fig. 4c), similar to the masses of SPESP1 isoforms in sperm (47 and 43 kDa). In addition, endo-α-*N*-acetylgalactosaminidase treatment abolished the 67-kDa band. Combined treatment with PNGase-F and neuraminidase resulted in mass shifts of SPESP1 immunoreactive bands to 70 kDa (neuraminidase) and 60 kDa (PNGase-F) (Fig. 4d). These mobility shifts were absent in buffer control (Fig. 4, lane −) testicular extracts not treated with deglycosidases.

Treatment of testicular proteins with a cocktail of deglycosylation enzymes containing PNGase-F, neuraminidase, endo-α-*N*-acetylgalactosaminidase (removes *O*-glycans), β1–4 galactosidase (releases only β1,4-linked, nonreducing terminal galactose), and β-*N*-acetylglucosaminidase (cleaves all nonreducing terminal β-linked *N*-acetylglucosamine residues) showed (Fig. 4e) a shift of all 77-kDa forms of SPESP1 to 70 kDa as well as the appearance of 60-, 55-, 50-, and 47-kDa forms, whereas the lower 67-kDa band

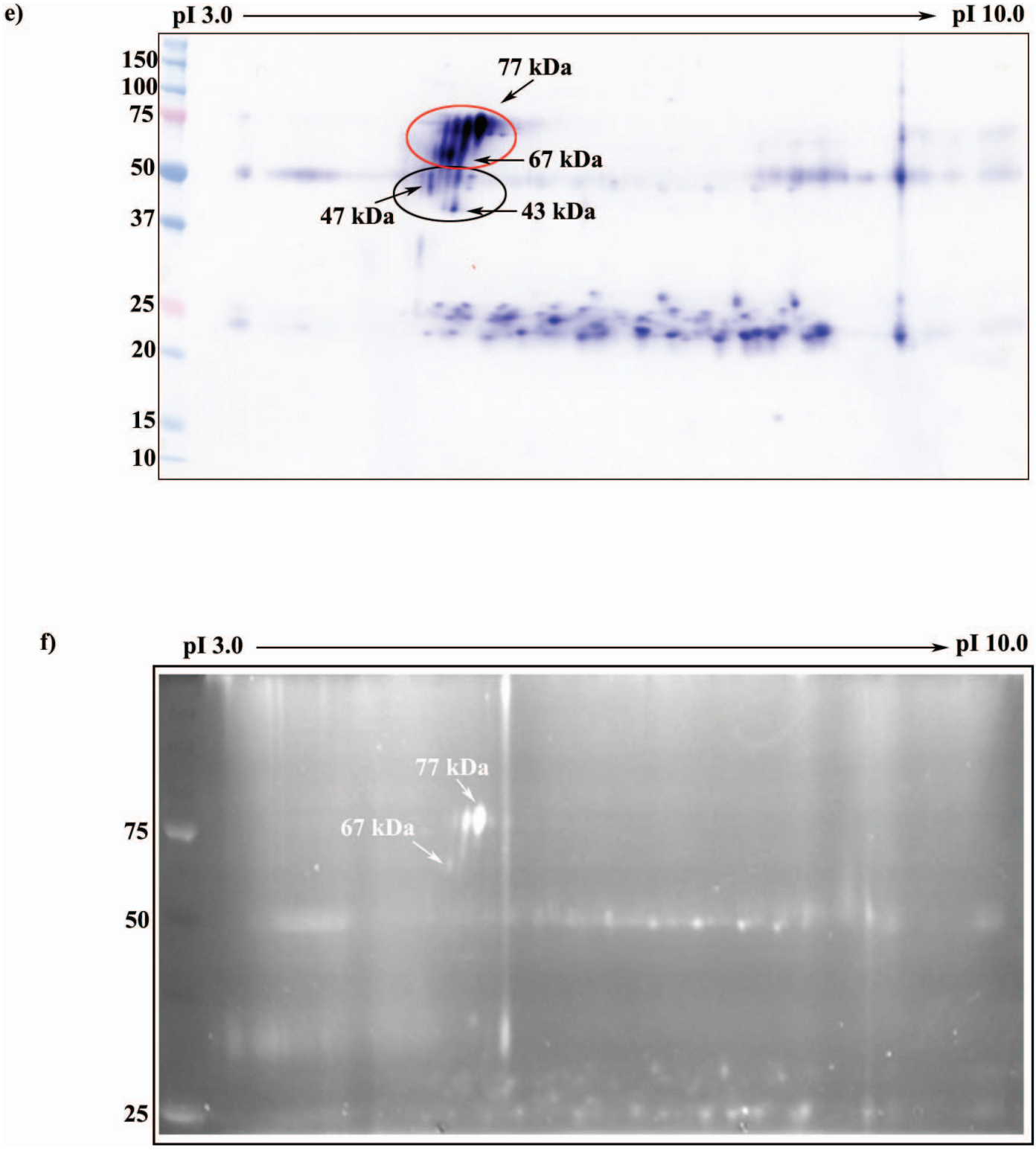

FIG. 3. *Continued*

completely vanished. Testis samples treated with buffer alone showed intact 77- and 67-kDa SPESP1 bands, confirming that the mobility shifts observed in samples treated with deglycosylation enzymes were due to removal of carbohydrate moieties, not to endogenous proteolysis (Fig. 4e). In sum, the 70-kDa SPESP1 band was a deglycosylation product of neuraminidase, the 60-kDa form was a PNGase-F deglycosylation product, and the 50-, 47-, and 43-kDa bands were deglycosylation products of endo-α-*N*-acetylgalactosaminidase.

Western blots of caudal sperm extracts treated with PNGase-F showed some evidence of deglycosylation. Although very little change was seen in the parent 47- and 43-kDa molecules, a 30-kDa immunoreactive SPESP1 band was

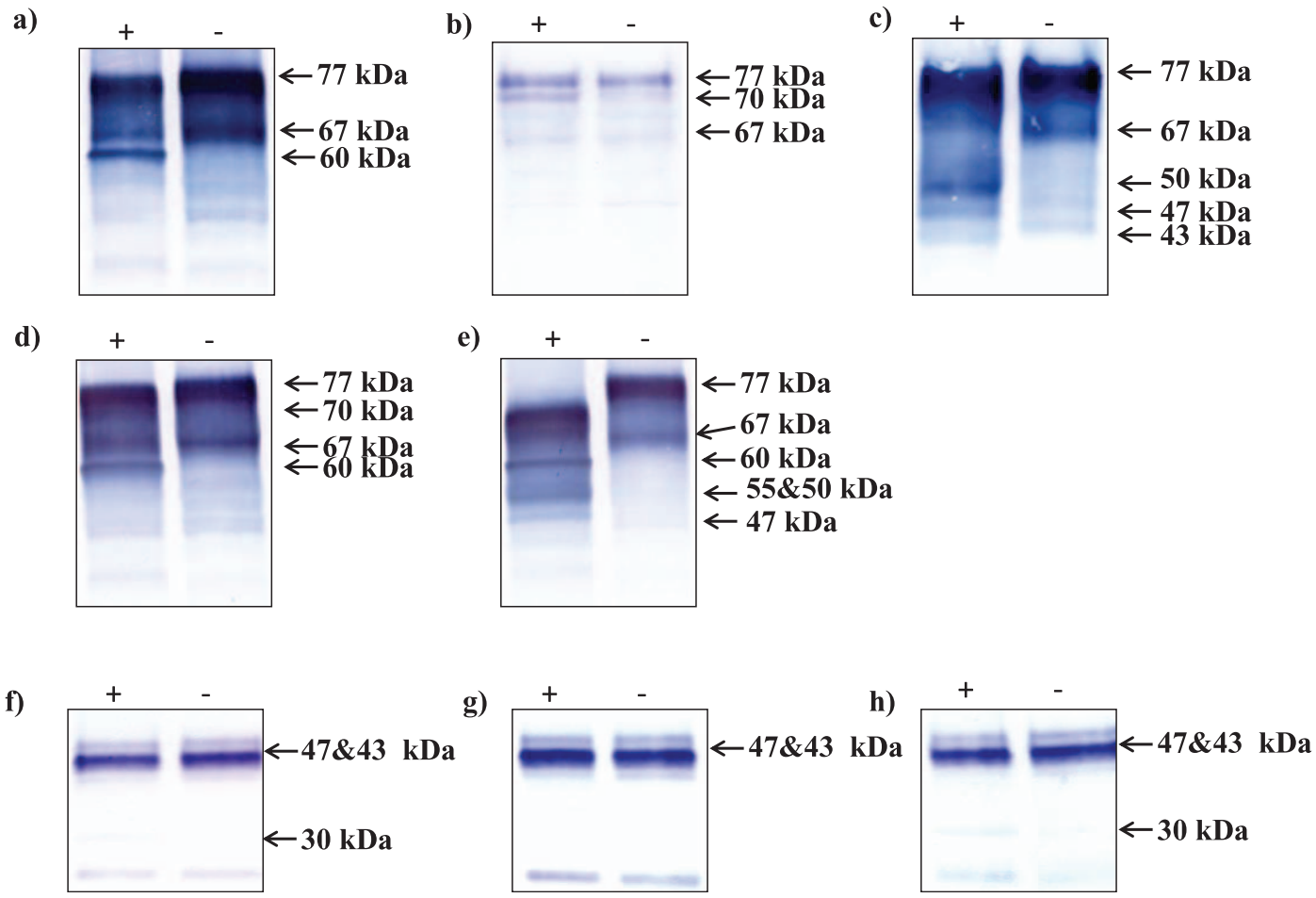

FIG. 4. Western blots of mouse testicular (**a**–**e**) and sperm (**f**–**h**) protein extracts treated with deglycosidases (+) or buffer alone (–) and stained with antibodies to SPESP1: PNGase-F (**a** and **f**), neuraminidase (**b** and **g**), endo-α-*N*-acetylgalactosaminidase (**c**), combination of PNGase-F and neuraminidase (**d** and **h**), and mixture of deglycosidases (**e**). Deglycosylated testicular SPESP1 showed major mass shifts, particularly with mixtures of deglycosidases (**e**), indicating testicular SPESP1 is highly glycosylated.

noted in the enzyme-treated, but not in the buffer-treated, samples (Fig. 4f). Neuraminidase-treated sperm extract did not show any deglycosylation-related mass changes (Fig. 4g). The combination of PNGase-F and neuraminidase also showed only one deglycosylated immunoreactive SPESP1 band at 30 kDa, which was absent in the buffer-treated sample (Fig. 4h). Given the repeated appearance of the 30-kDa SPESP1 band in caudal epididymal sperm extracts treated with PNGase-F and the known specificity of this amidase for cleaving between the innermost GlcNAc and asparagine residues of *N*-linked oligosaccharides, we conclude that caudal epididymal sperm SPESP1 contain an *N*-linked carbohydrate chain.

Determination of Possible Glycosylation Sites by Mass Spectrometry

The Expasy posttranslational modification analysis tool [35] predicted two *N*-linked glycosylation sites at amino acids 128 and 278 (NXS/T) in SPESP1 (N128 with high score and N278 with low score). Deamidation of asparagine to aspartic acid is a potential predictor of glycosylation sites [36, 37]. Mass spectrometry identified the peptide ISNINAEIQQGLLGGnNSPEFK with amino acid 278 shown to be deamidated, suggesting glycosylation at this classical consensus glycosylation sequence (NXS/T) in SPESP1. Strikingly, protein sequence analysis by mass spectrometry identified several additional potential *N*-glycosylation

TABLE 1. Summary of SPESP1 peptides showing deamidation in testis and sperm by mass spectrometry.

Sample	SPESP1 Peptides	Modifications
Testis	322-TSDPDNDmEmIInmLYNSR-340	N334 deamidated
Testis	322-TSDPDNDmEmIINmLYnSR-340	N338 deamidated
Testis	384-KLLS[nn]mK-391	N388 or N389 deamidated
Testis	263-ISNINAEIQQGLLGGnNSPEFK-284	N278 deamidated
Testis	263-ISNInAEIQQGLLGGNNSPEFK-284	N267 deamidated
Testis	263-ISNINAEIQQGLLGGNnSPEFK-284	N279 or N278 deamidated
Testis	384-KLLSNnMK-391	N389 deamidated
Sperm	197-ISSMATQPAnTQATR-211	N206 deamidated

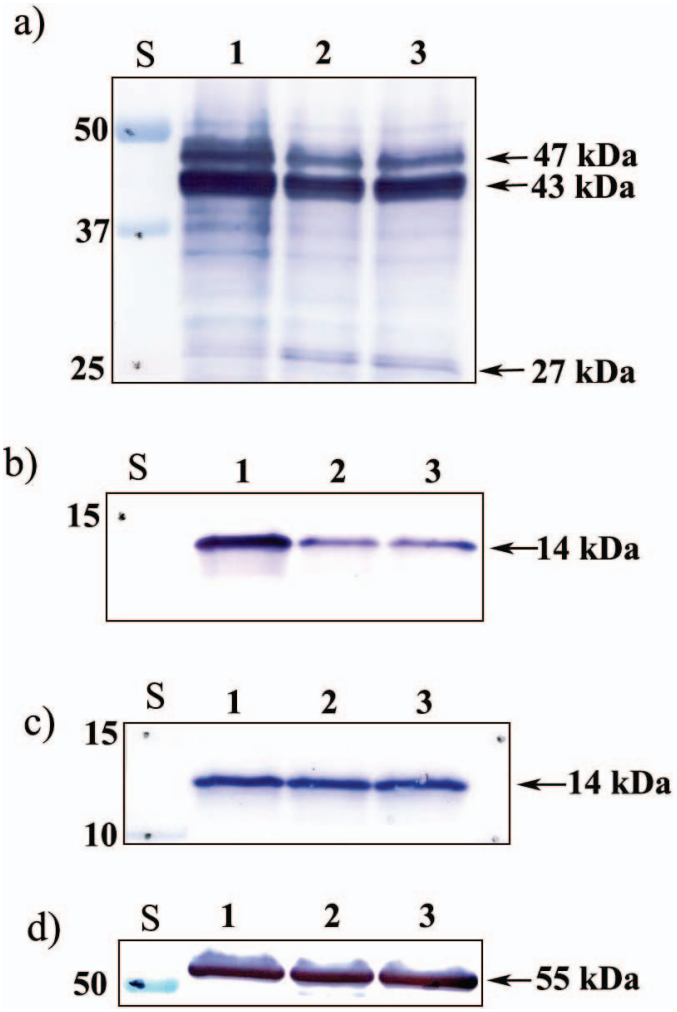

FIG. 5. Western blot analysis of intra-acrosomal proteins SPESP1, SLLP1, and SAMP14 during capacitation. Noncapacitated (0 h, lane 1), capacitated (90 min, lane 2) and capacitated, ionophore (A23187)-treated, and acrosome-reacted (for 30 min, lane 3) sperm were analyzed with antibodies to SPESP1 (**a**), SLLP1 (**b**), SAMP14 (**c**), and equal loading control beta-tubulin (**d**). A 27-kDa SPESP1 peptide appeared after capacitation only in SPESP1 samples. S, standard.

sites, further suggesting that SPESP1 is a glycoprotein (Table 1) and that multiple noncanonical asparagine residues may be involved. These include asparagine residues at 267, 279, and 338 (observed in three separate mass spectrometry experiments) as well as those at 388, 278, 334, and 389 (observed in two independent experiments). These observations included deamidations of the SPESP1 peptides ISNInAEIQQGLLGGNNSPEFK (n = 267), ISNINAEIQQGLLGGnNSPEFK (n = 278; predicted by Expasy glycosylation tool [Supplemental Fig. S3]; http://www.cbs.dtu.dk/services/NetNGlyc/), TSDPDNDmEmIInmLYNSR (n = 334), TSDPDNDMEMIINmLYnSR (n = 338), KLLSNnMK (n = 389), and KLLS[nn]mK (n = 388 and 389). Two of these noncanonical glycosylation sites have serine located adjacent to the asparagines (nS), whereas three showed methionines (nM or nm) next to the asparagines (Table 1).

Immunoprecipitation of caudal sperm SPESP1 showed 47- and 43-kDa immunoreactive bands and also a few additional bands of 37, 34, and 27 kDa (Fig. 3b). Analysis by mass spectrometry of 47-, 43-, 37-, and 34-kDa bands yielded 4, 12, 6, and 4 SPESP1 peptides, respectively. In contrast to the identification of numerous aspartic acid residues in testicular SPESP1, only one peptide, ISSMATQPAnTQATR, isolated from immunoprecipitated sperm SPESP1 showed deamidated N residues, in this case at residue 206 (Table 1).

SPESP1 Undergoes Further Changes During Capacitation

Mouse caudal epididymal sperm were collected in noncapacitation medium and capacitated for 90 min in WH medium, after which the acrosome reaction was induced with calcium ionophore A23187 for 30 min. SPESP1 isoforms in each group were subsequently examined by Western blot analysis (Fig. 5a). All three experimental samples showed prominent 47- and 43-kDa SPESP1 bands, with the 43-kDa band being more intense than the 47-kDa band, which ran as a tight doublet. The capacitated and acrosome-reacted samples revealed an additional 27-kDa immunoreactive band (Fig. 5a) that was very faint in the noncapacitated sperm. In capacitated as well as ionophore-treated spermatozoa, the upper band of the 47-kDa doublet showed decreased intensity, but little change was observed in the 43-kDa band, suggesting that the 27-kDa band might be derived from the upper 47-kDa doublet band. Duplicate membranes were probed with antibodies to other intra-acrosomal proteins, including anti-SLLP1 (an intra-acrosomal matrix protein) (Fig. 5b) [28] and anti-SAMP14 (an intra-acrosomal membrane protein) (Fig. 5c) [38]. Neither of these intra-acrosomal proteins showed additional lower-molecular-weight bands when capacitated and acrosome-reacted samples were compared to noncapacitated spermatozoa. Thus, a mass change during capacitation and the acrosome reaction is a feature that SPESP1 apparently does not share with these other intra-acrosomal proteins. It is tempting to speculate that this property of serving as a substrate for proteolysis during capacitation and the acrosome reaction may, in some way, relate to the restricted localization of SPESP1 to the equatorial segment subdomain and processes occurring there. However, due to unknown antibody coverage of SAMP14 and SLLP1 epitopes, peptide products of these proteins may have been undetected. A blot probed with a tubulin antibody confirmed the equal loading of these protein preparations (Fig. 5d).

Immunolocalization of SPESP1 in Noncapacitated and Capacitated Mouse Sperm

Immunofluorescent localization on fixed and permeabilized mouse sperm using the guinea pig anti-SPESP1 antibody revealed that SPESP1 was localized only in the equatorial segment (Fig. 6a). Both noncapacitated and capacitated, acrosome-reacted spermatozoa (lectin positive and negative, respectively) retained the SPESP1 proteins in the equatorial segment (Fig. 6b). Of 400 sperm scored for the acrosome reaction due to a lack of PNA staining of the anterior acrosome, 100% showed retention of SPESP1 in the equatorial segment. The nonimmune control serum did not stain the sperm (Supplemental Fig. S5, a1–a6). Comparison of the fluorescent-staining intensity of intact sperm with that of acrosome-reacted sperm revealed that the SPESP1 staining in acrosome-reacted sperm was less than in intact sperm. This suggested that although a population of SPESP1 is retained within all sperm after the acrosome reaction, some SPESP1 is lost from the equatorial segment with the acrosome reaction.

Live sperm (unfixed and nonpermeabilized) staining showed that SPESP1 protein was localized in the equatorial segments of 97% of sperm that had acrosome reacted and completely lost the anterior acrosome (Fig. 6c) as assessed by PNA lectin staining. Spermatozoa incubated with nonimmune

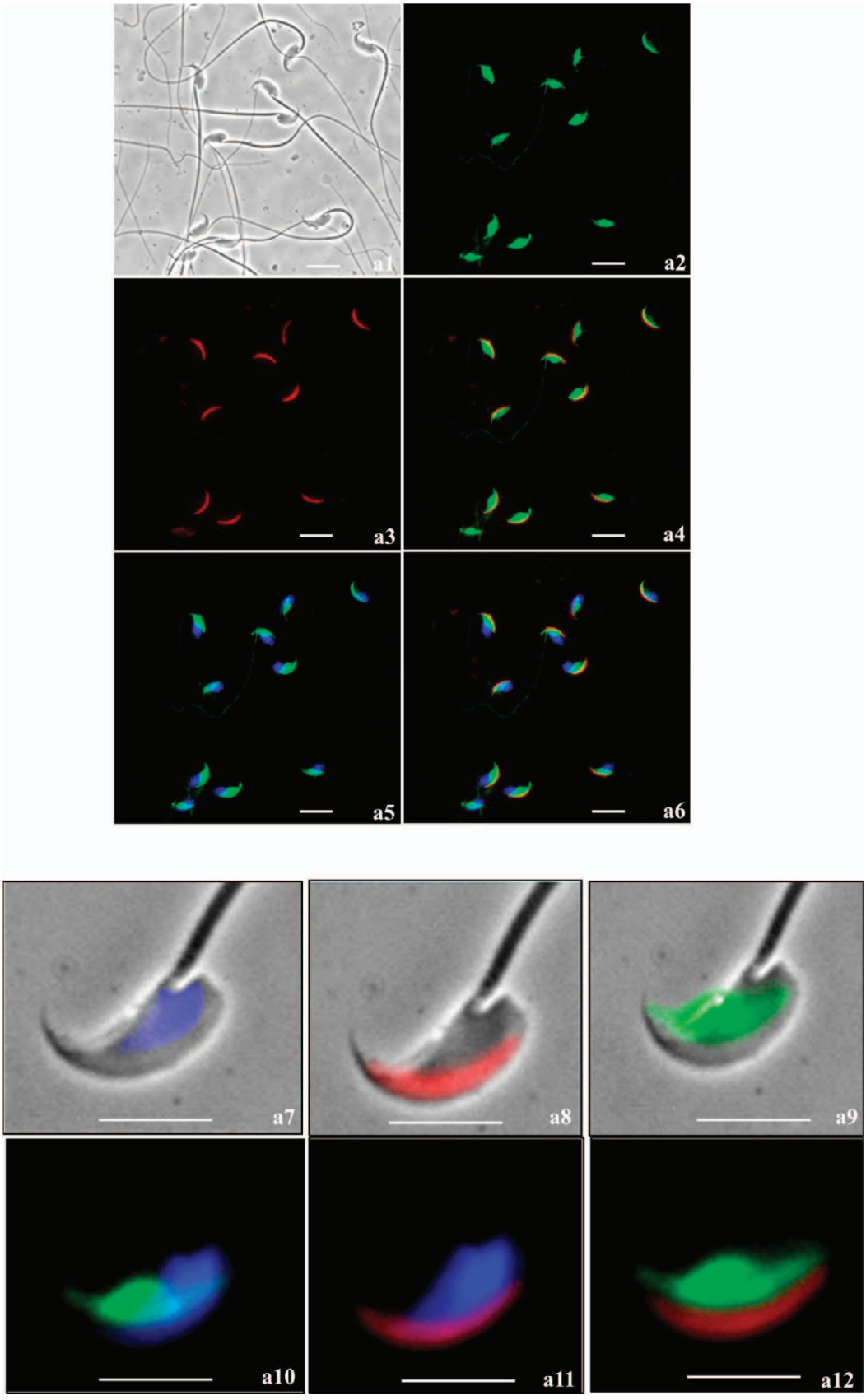

FIG. 6. Immunofluorescence analysis of SPESP1 (green signal) in fixed, permeabilized, noncapacitated (**a**) and capacitated, acrosome-reacted (**b**) spermatozoa. Noncapacitated spermatozoa and acrosome-reacted spermatozoa both retained SPESP1 immunofluorescence, which was confined to the equatorial segment. Status and position of the anterior acrosome was imaged using PNA lectin (red signal). **a**) Noncapacitated sperm: **a1**) bright field; **a2**) SPESP1 immunofluorescence confined to equatorial segment; **a3**) PNA staining of anterior acrosome; **a4**) merged image of PNA-positive anterior acrosome and SPESP1-positive equatorial segment demonstrating distinct domains; **a5**) green SPESP1domain overlain by blue 4′,6-diamidino-2-phenylindole (DAPI) nuclear staining; **a6**) merged image of SPESP1, PNA, and DAPI domains; **a7**) dual bright-field/fluorescence images of blue DAPI-

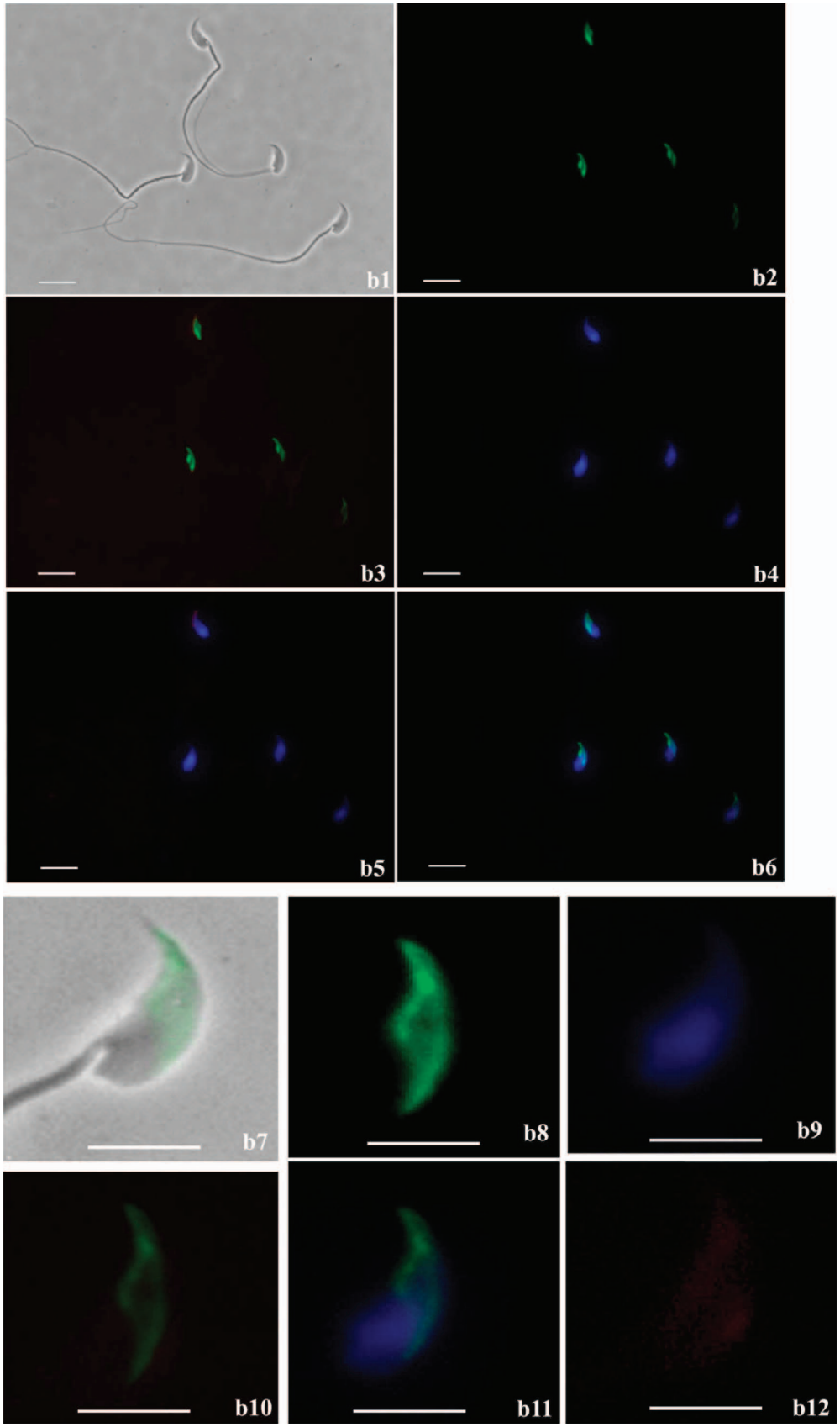

FIG. 6. *Continued*.
stained sperm nucleus; **a8**) dual bright-field/fluorescence image of PNA-stained anterior acrosome; **a9**) dual bright-field/fluorescence image of SPESP1-positive domain confined to equatorial segment; **a10**) dual SPESP1 and DAPI; **a11**) dual DAPI and PNA; **a12**) dual SPESP1 and PNA-positive revealing distinct segregation of PNA and SPESP1 domains. Bar = 10 μm (**a1**–**a6**) and 5 μm (**a7**–**a12**). **b**) Capacitated, acrosome-reacted sperm: **b1**) bright field; **b2**) green immunofluorescent SPESP1 domain confined to equatorial segment in each cell, albeit at lower intensity than in acrosome-intact sperm (**a** series above); **b3**) SPESP1 and PNA staining reveals absence of red staining anterior acrosome in acrosome-reacted sperm; **b4**) DAPI staining alone; **b5**) DAPI

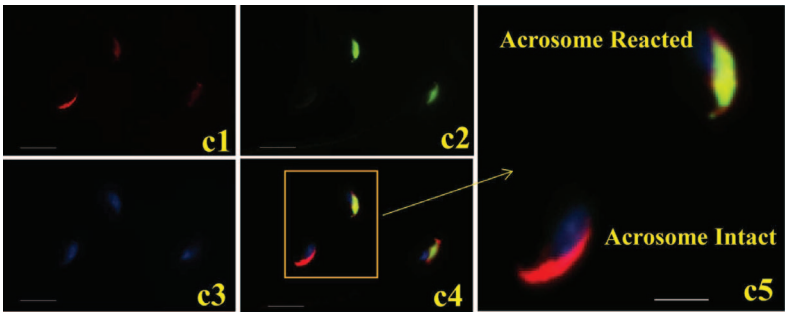

FIG. 6. *Continued.*
and PNA; **b6**) SPESP1, PNA, and DAPI; **b7**) dual bright-field/fluorescence of SPESP1 domain in acrosome-reacted sperm lacking anterior acrosome; **b8**) SPESP1 domain in acrosome-reacted sperm; **b9**) DAPI; **b10**) dual SPESP1 and PNA; **b11**) dual SPESP1 and DAPI; **b12**) SPESP1, PNA, and DAPI. Bar = 10 μm (**b1**–**b6**) and 5 μm (**b7**–**b12**). **c**) Immunofluorescence localization of SPESP1 (green) in live stained acrosome-intact and acrosome-reacted epididymal sperm costained with PNA lectin (red) to determine acrosomal status: **c1**) PNA signals in sperm with and without acrosomes; **c2**) SPESP1 localization within the equatorial segment domain in sperm that had undergone the acrosome reaction and lost the anterior acrosome; **c3**) DAPI signal for DNA in nucleus; **c4**) merged image of SPESP1 localization in the equatorial segment; **c5**) inset showing magnified region of **c4**. Bar = 10 μm (**c1**–**c5**) and 5 μm (**c5**).

serum showed no positive immunofluorescent signals (Supplemental Fig. S6). This result indicates that SPESP1 is retained in the equatorial segment of acrosome-reacted live sperm. However, it does not definitively assign the localization of the equatorial segment domain-restricted SPESP1 to the plasma membrane overlying the equatorial segment, to intra-acrosomal SPESP1 lying within the acrosomal matrix between the inner and outer acrosomal membranes, or to both the plasma membrane overlying the equatorial segment and an intra-acrosomal site. This is because the acrosomal matrix becomes accessible (to antibody and other molecular interactions) via the cleft created by the loss of the anterior acrosome and accompanying outer acrosomal membrane. Thus, from these light-microscopic observations alone, it is not certain if intra-acrosomal SPESP1 translocates to the plasma membrane overlying the equatorial segment, as has been suggested for MN9 [21]. A definitive resolution to this question requires detailed ultrastructural immunolocalization studies of the plasmalemma overlying the equatorial segment using probes for both MN9 and SPESP1.

Mouse SPESP1 Has Complementary Binding Sites on Unfertilized Zona-Free Eggs

To study the possible localization of mSPESP1-binding sites on the egg surface, unfertilized zona-free oocytes were incubated with purified recSPESP1 for 60 min, washed, and then exposed to anti-recSPESP1. Unfertilized oocytes exhibited fluorescent labeling of SPESP1 within the microvillar domain of the oocyte surface (Fig. 7), which lies antipodal to the eccentrically located meiotic-arrested oocyte nucleus. An area devoid of fluorescence on the oocyte surface was consistently detected, and Hoechst staining (Fig. 7b) revealed that this negative area was always associated with the nonmicrovillar area of the oocyte's plasma membrane overlying the metaphase plate (Fig. 7). Thus, mSPESP1-binding sites were restricted to the fusogenic region of the egg, consistent with a role for SPESP1 interaction in sperm–egg binding [7]. Oocytes incubated with nonimmune serum, BSA (negative control), or medium alone (no protein control) did not show any immunoreactivity (data not shown).

recSPESP1 and Anti-recSPESP1 Serum Inhibited IVF

To determine a possible role of SPESP1 during mouse fertilization, both spermatozoa and zona-intact oocytes were preincubated with anti-recSPESP1 serum or nonimmune serum for 60 min before insemination. Fertilization was conducted in the presence of the antibody, and 6 h later, the eggs were washed with fertilization medium and incubated overnight. With immune sera (1:50 dilution), the percentage of 2-cell embryos was reduced (37%) compared to that with nonimmune serum. Incubation of oocytes with recSPESP1 protein also inhibited fertilization by 50% compared to BSA incubation or no-protein controls. These data suggest that the SPESP1 molecule is, in part, involved in fertilization (data not shown).

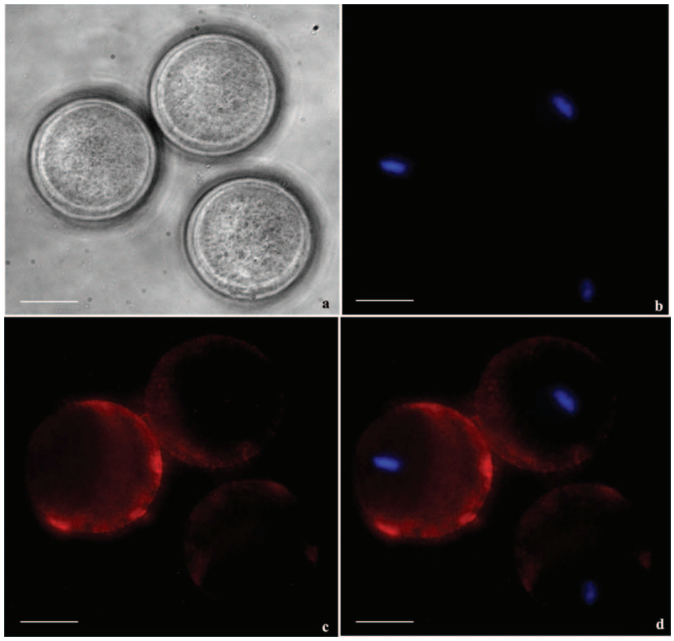

FIG. 7. Zona-free mouse oocytes were incubated with recSPESP1 protein and probed with SPESP1 immune and nonimmune antibody to detect the oolemmal binding domain of SPESP1. Bright field (**a**), nuclear 4′,6-diamidino-2-phenylindole (DAPI) stain in blue (**b**), immune SPESP1 in red (**c**), and overlapped image (**d**) revealed SPESP1 binding to microvillar domain antipodal to eccentrically located M2 nucleus. Bar = 25 μm.

DISCUSSION

Changes in Mass of 77- and 67-kDa Testicular SPESP1 Occur Before Sperm Arrive in the Caput Epididymis

Mass spectrometry analysis of both high- and low-molecular-weight immunoreactive bands and spots from 1D and 2D Western blots recovered multiple SPESP1 peptides, confirming that the proteins studied in this report represent authentic SPESP1 isoforms, validating the specificity of the antiserum employed, and revealing microheterogeneity of SPESP1 in both testis and sperm. The analysis of sperm proteins from the caput, corpus, and cauda epididymis revealed that none of these epididymal samples contained the 77- or 67-kDa SPESP1 isoforms that were seen in testis. This finding indicated that the transformation of SPESP1 from high-molecular-weight, 77/67-kDa to lower-molecular-weight, 47/43-kDa isoforms occurred before sperm reached the caput epididymis. That this transformation in mass is already underway in the testis is supported by detection of a minor subpopulation of 47- and 43-kDa SPESP1 in testicular protein extracts in addition to the major testicular 77- and 67-kDa SPESP1 forms. The array of SPESP1 bands (47 and 43 kDa) in epididymal samples did not show any major molecular weight differences in samples from different epididymal regions, suggesting that SPESP1 had undergone posttranslational changes within the seminiferous epithelium before spermiation, within the lumen of the seminiferous tubules, in the rete testis, or in the efferent ductules before entering the epididymis. The relative intensities of immunoreactive SPESP1 bands did vary in the samples from caput, corpus, and cauda (Fig. 2), although equal amounts of proteins were loaded in each well. These differences may reflect regional sperm densities.

Testicular SPESP1 Is Glycosylated

Four lines of evidence support the hypothesis that 77- and 67-kDa SPESP1 isoforms in the testis are highly glycosylated. First, the 77-kDa band and 77- and 67-kDa SPESP1 spots recovered from the testis by immunoprecipitation stained with the glycoprofile stain. Second, the 77- and 67-kDa protein bands and spots staining with glycoprofile were confirmed to be authentic SPESP1 by Western blot analysis with SPESP1 antibody and by identification of SPESP1 peptides (77 kDa) by mass spectrometry microsequencing. Third, the 77- and 67-kDa SPESP1 isoforms decreased in apparent mass after enzymatic deglycosylation. Fourth, deamidated asparagine residues (N = 334, 338, 388, 278, 267, 279/278, and 389) were present in the testicular SPESP1 peptides (eight sites), whereas only one site was found in the sperm SPESP1 peptides (N = 206), suggesting that a subpopulation of asparagine residues in the high-molecular-weight forms of SPESP1 had been converted to aspartic acid in the testis samples (Table 1).

Glycosylation site prediction programs showed a potential glycosylated site at amino acid 128 (Supplemental Fig. S3). Mass spectrometry data could not confirm this site due to failure to recover tryptic peptides between amino acids 1–134, although this region contains several potential tryptic arginine and lysine residues (Supplemental Fig. S2). It is possible that glycosylation protects this region from tryptic hydrolysis.

Deglycosylation with a deglycosidase mixture resulted in reductions in mass of both 77- and 67-kDa bands (Fig. 4e). The 67-kDa SPESP1 showed only one glycoprofile positive spot on 2D gels (Fig. 3f) and may be less sensitive to glycoprofile stain.

77- and 67-kDa Testicular SPESP1 Isoforms Are Polyglycosylated Sialoglycoproteins

Deglycosylation with various glycosidases that trim complex carbohydrate chains at various linkages confirmed that glycosylation of the 77- and 67-kDa testicular isoforms of SPESP1 involves both *N*- and *O*-linked sugars as well as sialic acid. Neuraminidase removal of sialic acid, which is usually terminal on carbohydrate chains, resulted in a 7-kDa mass shift from 77 to 70 kDa, suggesting that SPESP1 is a highly sialylated or polysialylated protein. PNGase-F treatment is known to release *N*-linked carbohydrates [39], and treatment of testicular SPESP1 with PNGase-F resulted in 17-kDa mass shifts, indicating that a population of SPESP1 contains *N*-linked sugars. Removal of *O*-linked *N*-acetyl galactosamine with endo-α-*N*-acetylgalactosaminidase caused the 77- and 67-kDa testicular SPESP1 to shift to 50-, 47-, and 43-kDa bands (Fig. 4c), similar to the masses of SPESP1 isoforms in sperm (47 and 43 kDa), indicating that a subpopulation of testicular SPESP1 contains *O*-linked carbohydrates and that these glycosidic linkages are very abundant. Bioinformatic analysis predicts 18 *O*-linked and 2 canonical *N*-linked glycosylation sites in SPESP1. Preliminary analysis by mass spectrometry of testicular SPESP1 identified deamidated asparagines at one canonical NXS/T site (N = 278) (Supplemental Fig. S3), which was also predicted by Expasy tool, and five noncanonical sites, including two sites having serine located next to the asparagines (NS) and three sites showing methionines next to the asparagines (NM). Similar noncanonical glycosylation sites have been identified by mass spectrometry in breast cancer cell lines [36]. Analysis of *O*-glycosylation by mass spectrometry of peptides is a difficult task because of high structural diversity of glycans, including the carbohydrate moiety mediating attachment and nature of sugar backbone molecules [40]. Further studies are needed to identify the type, sequences, and branching of these carbohydrate chains. This evidence for SPESP1 glycosylation is in concert with the observation that the high-molecular-weight forms of murine testicular SPESP1 run on gels as a smear between 77 and 67 kDa.

Microheterogeneity of Mouse Sperm SPESP1

In addition to discovering the glycosylated testicular isoforms of SPESP1, the present study refines and enlarges previous reports [6, 7] that characterized mouse sperm SPESP1. The present findings define mouse sperm SPESP1 as a microheterogeneous protein with two predominant 47- and 43-kDa isoforms. Fujihara et al. [7] reported mouse sperm SPESP1 as a 40-kDa protein [7]. Lv et al. [6] found SPESP1 to be a 45-kDa protein. Although a major loss of carbohydrate from SPESP1 appears to occur in the testis, some glycoconjugates of mouse SPESP1 are retained in sperm. No mass shifts in mouse cauda sperm SPESP1 were observed after treatments with the deglycosidase neuraminidase; however, PNGase-F treatment resulted in the appearance of a faint 30-kDa band (17-kDa shift), indicating that some *N*-glycosylation-linked glycoconjugates of sperm SPESP1 persist. This supports earlier findings in humans [5] that ejaculated sperm SPESP1 bound PSA lectin.

Proteolysis of SPESP1 Occurs During Capacitation and the Acrosome Reaction

The comparison of noncapacitated (0 min), capacitated (90 min), and capacitated, acrosome-reacted spermatozoa (120 min) showed SPESP1 mass changes during capacitation and

the acrosome reaction. In noncapacitated spermatozoa, 47- and 43-kDa SPESP1-positive bands predominated, with two minor bands at 37 and 34 kDa. Capacitated, acrosome-reacted samples of SPESP1 showed 47- and 43-kDa bands and an additional SPESP1-positive band at 27 kDa, suggesting that SPESP1 underwent proteolysis during capacitation and the acrosome reaction. The identical samples were examined for mass shifts in other sperm-specific, intra-acrosomal antigens, such SLLP1 [28] and SAMP14 [38], but these proteins did not show the appearance of lower-molecular-weight products.

SPESP1 Is Retained in the Equatorial Segment of Acrosome-Reacted Mouse Sperm

Fujihara et al. [7] reported that SPESP1 was detected in mouse sperm only after membrane permeabilization, a finding supported by the present study in mice as well as previous results in human sperm [4]. All published reports agree that SPESP1 is restricted to the intra-acrosomal equatorial segment compartment of noncapacitated caudal sperm. The present findings differ notably from those of Fujihara et al. [7], however, regarding the fate of SPESP1 after capacitation and the acrosome reaction. Based on the use of anti-SPESP1 peptide antisera, Fujihara et al. concluded that when sperm underwent the acrosome reaction, SPESP1 was no longer detected in the equatorial segment. The present study examined 400 ionophore-induced acrosome-reacted mouse sperm, each validated to be acrosome reacted by the absence of PNA lectin stain of the anterior acrosome, and we observed SPESP1 to be retained and confined in the equatorial segment of all, using an anti-recombinant full-length SPESP1 immunoreagent. Appreciation that SPESP1 is retained in the equatorial segment of acrosome-reacted sperm is crucial for a complete understanding of SPESP1's biological role and supports the interpretation that this molecule plays an important role in equatorial segment structural integrity [7]. Comparison of intact mouse sperm with acrosome-reacted sperm by Western blot analysis (Fig. 5a) showed that the 43-kDa isoform of SPESP1 was maintained in acrosome-reacted sperm whereas the 47-kDa isoform was reduced, leading to the hypothesis that the 43-kDa isoform may be the SPESP1 isoform that is retained within the equatorial segment and mediates the tight binding that occurs between the leaflets of the inner and outer acrosomal membranes characterizing the equatorial segment in the region of tight apposition. Studies of SPESP1 in the equatorial segment of acrosome-reacted human sperm [5] similarly show retention within the equatorial segment, albeit with a lower intensity of SPESP1 staining.

SPESP1 Glycosylation Is Germane to Understanding SPESP1's Role in Acrosome Biogenesis and Fertilization

The murine knockout (KO) of SPESP1 showed reduced average litter size from 10 to 7.8 pups (but not complete infertility) as well as dramatic changes in sperm-egg fusion during IVF (from 4.2 to 1.9 sperm/egg) and a decrease in IVF rates (from 90% to 37.2%) [7]. In the present study, both anti-mouse SPESP1 immune sera and recSPESP1 protein reduced the percentage of 2-cell embryos when compared to control, underscoring that the SPESP1 molecule is involved in fertilization. Zona-intact oocytes incubated with anti-ESP antibody showed 60% inhibition of fertilization in mice [6], and antibodies to hSPESP1 blocked the hamster egg penetration test by 52% [5]. SPESP1 thus has been shown to play a role in fertilization, albeit one that is not entirely indispensable, and this role may, in part, be compensated by other proteins. It is well established that sperm fuse in the microvillar region of the murine egg (see Figure 1 in Runge et al. [41]). Mouse recSPESP1 incubated with zona-free oocytes showed microvillar domain binding antipodal to the position of the metaphase II-arrested nucleus, supporting a role for SPESP1 in sperm-oocyte fusion. This observation of microvillar domain binding of SPESP1 contrasts with a previous study that found recSPESP1 protein binding across the entire oocyte surface [6]. In addition, acrosome-reacted sperm isolated by cell sorting from SPESP1 KO mice show a loss of the plasma membrane that overlies the equatorial segment all the way back to the edge of the equatorial segment domain in scanning microscopic images of freeze-dried sperm [7], providing direct evidence that SPESP1 plays a role in maintaining the integrity of the equatorial segment domain of the plasma membrane. Thus, the microheterogeneity and glycosylation of SPESP1 protein isoforms are germane to understanding both the role of SPESP1 in acrosome biogenesis, particularly equatorial segment formation, and the role of the equatorial segment in fertilization, including equatorial segment preservation and integrity after the acrosome reaction.

New Hypotheses Emerging from These Findings

The finding of a 77/67- to 47/43-kDa transformation in SPESP1 mass within the testis leads to new hypotheses regarding acrosome biogenesis. The first hypothesis is that deglycosylation of some acrosomal matrix proteins accompanies acrosome biogenesis and equatorial segment formation. SPESP1 has been shown to appear as early as the Golgi phase in the electron-lucent regions of the acrosomal vesicle matrix and to mark an intra-acrosomal equatorial segment domain during cap and elongation phases of acrosome formation [4]. SPESP1 then localizes within the equatorial segment of mature sperm. The hypothesis that deglycosylation of SPESP1 accompanies equatorial segment formation opens a potentially new and exciting field of enquiry into the molecular events underlying aspects of acrosomal biogenesis that have previously received scant attention—namely, acrosomal matrix condensation and formation of the bridges between inner and outer acrosomal membranes that stabilize and characterize the equatorial segment. Because the acrosome is considered a hybrid organelle orthologous to both secretory granules and lysosomes [3, 42, 43], the hypothesis that deglycosylation of acrosomal matrix components accompanies acrosome biogenesis may be of general cell biological significance when considering the phenomenon of secretory granule condensation, which occurs in a variety of exocrine cells. To our knowledge, mass changes of acrosomal matrix proteins ascribed to deglycosylation have not been previously proposed to occur during spermiogenesis. However, the sperm equatorial region protein equatorin, also a glycoprotein, showed a pattern of deglycosylation during epididymal maturation [44].

A second proposition arising from the present study is that SPESP1 glycosylation and deglycosylation are both occurring within the testis. This suggests that SPESP1 is possibly glycosylated during early spermiogenesis and then subsequently deglycosylated, likely before spermatid release as acrosome formation is completed. A central question is whether glycosylation and deglycosylation occur within the Golgi during synthesis of proacrosomal granules or within the acrosomal vesicle itself. One corollary derived from the second hypothesis is that intra-acrosomal deglycosidases are predicted to be synthesized at some stage of acrosome biogenesis and become activated within the acrosomal vesicle or acrosomal membranes. Due to the observation that 18 *O*-linked

glycosylation sites are predicted in SPESP1 and that the *O*-glycosidase β1–4-*N*-acetylgalactosaminidase effected the most significant reduction in mass of testicular SPESP1, this corollary leads to a prediction that an *O*-glycosidase is involved in modification of SPESP1 during acrosome biogenesis. A second corollary posits that the deglycosylation of SPESP1 is achieved by proteolytic removal of a highly glycosylated peptide fragment of SPESP1. Failure to recover peptides by tryptic digestion and mass spectrometry within the C-terminal 29 amino acids of sperm SPESP1 may indicate sperm SPESP1 lacks this region and a highly glycosylated peptide lies therein that is removed by a carboxypeptidase. Possibly, deglycosidases and proteolysis act in concert to achieve the SPESP1 mass changes revealed in the present study.

During the various steps of acrosomal biogenesis, the acrosomal matrix undergoes condensation in a process that is analogous to the condensation of secretory granules destined for release by regulated exocytosis [45]. The condensation and packaging of secretory granule luminal proteins, where intragranular concentrations of 0.1 g/ml of a diverse array of secretory proteins coexist within a single granule, previously were ascribed to a variety of processes, including protein dimerization, removal of luminal contents from the immature granule by vesicular budding [46], proteolytic processing, changes in ionic environment including mild acidification, and ions such as zinc or calcium [45]. Such processes reflect progressive protein insolubility within the luminal environment of the maturing granule. To our knowledge, no previous author has suggested that protein glycosylation and deglycosylation may accompany secretory granule condensation. The acrosome in some respects represents a unique type of secretory granule in that the granule membranes (inner and outer acrosomal membranes) undergo adhesion during formation of the zone of tight apposition in the equatorial segment. It is possible that deglycosylation of SPESP1 represents a process unique to the formation of the equatorial segment. Alternatively, deglycosylation of secretory granule luminal proteins during secretory granule condensation may be a more widespread phenomenon occurring in other secretory cells.

ACKNOWLEDGMENT

The authors thank Mr. Ken Klotz, Prof. David Castle, and Drs. Kula N Jha, Arabinda Mandal, and Eusebio Pires for their critical suggestions. A special thanks to Dr. Manjeet Rao, Associate Professor, Greehey Children's Cancer Research Institute, University of Texas Health Science Center at San Antonio, San Antonio, Texas.

REFERENCES

1. Yanagimachi R, Noda YD. Physiological changes in the postnuclear cap region of mammalian spermatozoa: a necessary preliminary to the membrane fusion between sperm and egg cells. J Ultrastruct Res 1970; 31:486–493.
2. Bedford JM, Moore HD, Franklin LE. Significance of the equatorial segment of the acrosome of the spermatozoon in eutherian mammals. Exp Cell Res 1979; 119:119–126.
3. Yanagimachi R. Mammalian fertilization. In: Knobil E, Neill JD (eds.), The Physiology of Reproduction, vol 1, 2nd ed. New York: Raven Press; 1994:189–317.
4. Wolkowicz MJ, Shetty J, Westbrook A, Klotz K, Jayes F, Mandal A, Flickinger CJ, Herr JC. Equatorial segment protein defines a discrete acrosomal subcompartment persisting throughout acrosomal biogenesis. Biol Reprod 2003; 69:735–745.
5. Wolkowicz MJ, Digilio L, Klotz K, Shetty J, Flickinger CJ, Herr JC. Equatorial segment protein (ESP) is a human alloantigen involved in sperm-egg binding and fusion. J Androl 2008; 29:272–282.
6. Lv ZM, Wang M, Xu C. Antifertility characteristics of the N-terminal region of mouse equatorial segment protein. Anat Rec 2010; 13:605–613.
7. Fujihara Y, Murakami M, Inoue N, Satouh Y, Kaseda K, Ikawa M, Okabe M. Sperm equatorial segment protein 1, SPESP1, is required for fully fertile sperm in mouse. J Cell Sci 2010; 123:1531–1536.
8. Jones R, James PS, Oxley D, Coadwell J, Suzuki-Toyota F, Howes EA. The equatorial subsegment in mammalian spermatozoa is enriched in tyrosine phosphorylated proteins. Biol Reprod 2008; 79:421–431.
9. Suzuki F. Changes in intramembranous particle distribution in epididymal spermatozoa of the boar. Anat Rec 1981; 199:361–376.
10. Friend DS, Fawcett DW. Membrane differentiations in freeze-fractured mammalian sperm. J Cell Biol 1974; 63:641–664.
11. Phillips DM. Surface of the equatorial segment of the mammalian acrosome. Biol Reprod 1977; 16:128–137.
12. Ellis DJ, Shadan S, James PS, Henderson RM, Edwardson JM, Hutchings A, Jones R. Post-testicular development of a novel membrane substructure within the equatorial segment of ram, bull, boar, and goat spermatozoa as viewed by atomic force microscopy. J Struct Biol 2002; 138:187–198.
13. Yanagimachi R, Bhattacharyya A. Acrosome-reacted guinea pig spermatozoa become fusion competent in the presence of extracellular potassium ions. J Exp Zool 1988; 248:354–360.
14. Camatini M, Anelli G, Casale A. Immunocytochemical localization of calmodulin in intact and acrosome-reacted boar sperm. Eur J Cell Biol 1986; 41:89–96.
15. Camatini M, Casale A. Actin and calmodulin coexist in the equatorial segment of ejaculated boar sperm. Gamete Res 1987; 17:97–105.
16. Howes EA, Hurst SM, Jones R. Actin and actin-binding proteins in bovine spermatozoa: potential role in membrane remodelling and intracellular signalling during epididymal maturation and the acrosome reaction. J Androl 2001; 22:62–72.
17. Feinberg JM, Rainteau DP, Kaetzel MA, Dacheux JL, Dedman JR, Weinman SJ. Differential localization of annexins in ram germ cells: a biochemical and immunocytochemical study. J Histochem Cytochem 1991; 39:955–963.
18. Mitchell LA, Nixon B, Aitken RJ. Analysis of chaperone proteins associated with human spermatozoa during capacitation. Mol Hum Reprod 2007; 13:605–613.
19. Kamaruddin M, Kroetsch T, Basur PK, Hansen PJ, King WA. Immunolocalization of heat shock protein 70 in bovine spermatozoa. Andrologia 2004; 36:327–334.
20. Toshimori K, Tanii I, Araki S, Oura C. Characterization of the antigen recognized by a monoclonal antibody MN9: unique transport pathway to the equatorial segment of sperm head during spermiogenesis. Cell Tissue Res 1992; 270:459–468.
21. Toshimori K, Saxena DK, Tanii I, Yoshinaga K. An MN9 antigenic molecule, equatorin, is required for successful sperm-oocyte fusion in mice. Biol Reprod 1998; 59:22–29.
22. Yoshinaga K, Saxena DK, Oh-oka T, Tanii I, Toshimori K. Inhibition of mouse fertilization in vivo by intra-oviductal injection of an anti-equatorin monoclonal antibody. Reproduction 2001; 122:649–655.
23. Manandhar G, Toshimori K. Exposure of sperm head equatorin after acrosome reaction and its fate after fertilization in mice. Biol Reprod 2001; 65:1425–1436.
24. Jha KN, Shumilin IA, Digilio LC, Chertihin O, Zheng H, Schmitz G, Visconti PE, Flickinger CJ, Minor W, Herr JC. Biochemical and structural characterization of apolipoprotein A-I binding protein, a novel phosphoprotein with a potential role in sperm capacitation. Endocrinology 2008; 149:2108–2120.
25. Jha KN, Salicioni AM, Arcelay E, Chertihin O, Kumari S, Herr JC, Visconti PE. Evidence for the involvement of proline-directed serine/threonine phosphorylation in sperm capacitation. Mol Hum Reprod 2006; 12:781–789.
26. Visconti PE, Bailey JL, Moore GD, Pan D, Olds-Clarke P, Kopf GS. Capacitation of mouse spermatozoa. I. Correlation between the capacitation state and protein tyrosine phosphorylation. Development 1995; 121: 1129–1137.
27. Moore GD, Ayabe T, Visconti PE, Schultz RM, Kopf GS. Roles of heterotrimeric and monomeric G proteins in sperm-induced activation of mouse eggs. Development 1994; 120:3313–3323.
28. Herrero MB, Mandal A, Digilio LC, Coonrod SA, Maier B, Herr JC. Mouse SLLP1, a sperm lysozyme-like protein involved in sperm-egg binding and fertilization. Dev Biol 2005; 284:126–142.
29. Shetty J, Diekman AB, Jayes FC, Sherman NE, Naaby-Hansen S, Flickinger CJ, Herr JC. Differential extraction and enrichment of human sperm surface proteins in a proteome: identification of immunocontraceptive candidates. Electrophoresis 2001; 22:3053–3066.
30. Naaby-Hansen S, Flickinger CJ, Herr JC. Two-dimensional gel electrophoretic analysis of vectorially labeled surface proteins of human spermatozoa. Biol Reprod 1997; 56:771–778.

31. Nita-Lazar M, Wacker M, Schegg B, Amber S, Aebi M. The N-X-S/T consensus sequence is required but not sufficient for bacterial N-linked protein glycosylation. Glycobiology 2005; 15:361–367.
32. Mimura Y, Jefferis R, Mimura-Kimura Y, Abrahams J, Rudd P. Glycosylation of Therapeutic IgGs. In: An Z (ed.), Threrapeutic Monoclonal Antibodies: From Bench to Clinic. John Wiley & Sons: Hoboken, NJ; 2009:67–89.
33. Maley F, Trimble RB, Tarentino AL, Plummer TH Jr. Characterization of glycoproteins and their associated oligosaccharides through the use of endoglycosidases. Anal Biochem 1989; 180:195–204.
34. Uchida Y, Tsukada Y, Sugimori T. Enzymatic properties of neuraminidases from *Arthrobacter ureafaciens*. J Biochem 1979; 86:1573–1585.
35. Expasy Posttranslational Modification Analysis Tool, NetNGlyc [Internet]. Lyngby, Denmark: Center for Biological Sequence Analysis, Technical University of Denmark. http://www.cbs.dtu.dk/services/NetNGlyc/. Accessed February 16, 2010.
36. Whelan SA, Lu M, He J, Yan W, Saxton RE, Faull KF, Whitelegge JP, Chang HR. Mass spectrometry (LC-MS/MS) site-mapping of N-glycosylated membrane proteins for breast cancer biomarkers. J Proteome Res 2009; 8:4151–4160.
37. Khoshnoodi J, Hill S, Tryggvason K, Hudson B, Friedman DB. Identification of *N*-linked glycosylation sites in human nephrin using mass spectrometry. J Mass Spectrom 2007; 42:370–379.
38. Shetty J, Wolkowicz MJ, Digilio LC, Klotz KL, Jayes FL, Diekman AB, Westbrook VA, Farris EM, Hao Z, Coonrod SA, Flickinger CJ, Herr JC. SAMP14, a novel, acrosomal membrane-associated, glycosylphosphatidylinositol-anchored member of the Ly-6/urokinase-type plasminogen activator receptor superfamily with a role in sperm-egg interaction. J Biol Chem 2003; 278:30506–30515.
39. Tarentino AL, Gómez CM, Plummer TH Jr. Deglycosylation of asparagine-linked glycans by peptide: N-glycosidase F. Biochemistry 1985; 24:4665–4671.
40. Peter-Katalinic J. Methods in enzymology: O-glycosylation of proteins. Methods Enzymol 2005; 405:139–171.
41. Runge KE, Evans JE, He ZY, Gupta S, McDonald KL, Stahlberg H, Primakoff P, Myles DG. Oocyte CD9 is enriched on the microvillar membrane and required for normal microvillar shape and distribution. Dev Biol 2007; 304:317–325.
42. Chayko CA, Orgebin-Crist MC. Targeted disruption of the cation-dependent or cation-independent mannose 6-phosphate receptor does not decrease the content of acid glycosidases in the acrosome. J Androl 2000; 21:944–953.
43. Allison AC, Hartree EF. Lysosomal enzymes in the acrosome and their possible role in fertilization. J Reprod Fertil 1970; 21:501–515.
44. Yamatoya K, Yoshida K, Ito C, Maekawa M, Yanagida M, Takamori K, Ogawa H, Araki Y, Miyado K, Toyama Y, Toshimori K. Equatorin: identification and characterization of the epitope of the MN9 antibody in the mouse. Biol Reprod 2009; 81:889–897.
45. Arvan P, Castle D. Sorting and storage during secretory granule biogenesis: looking backward and looking forward. Biochem J 1998; 332:593–610.
46. Klumperman J, Kuliawat R, Griffith JM, Geuze HJ, Arvan P. Mannose 6-phosphate receptors are sorted from immature secretory granules via adaptor protein AP-1, clathrin, and syntaxin 6-positive vesicles. J Cell Biol 1998; 141:359–371.